ORIGINAL ARTICLE

DEVELOPMENTAL TRAIT EVOLUTION IN TRILOBITES

Giuseppe Fusco,[1] Theodore Garland, Jr.,[2] Gene Hunt,[3] and Nigel C. Hughes[4,5]

[1]Department of Biology, University of Padova, Italy

[2]Department of Biology, University of California, Riverside CA 92521

[3]Department of Paleobiology, National Museum of Natural History, Smithsonian Institution, Washington DC 20560

[4]Department of Earth Sciences, University of California, Riverside CA 92521

  [5]E-mail: nigel.hughes@ucr.edu

We performed a tree-based analysis of trilobite postembryonic development in a sample of 60 species for which quantitative data on segmentation and growth increments between putative successive instars are available, and that spans much of the temporal, phylogenetic, and habitat range of the group. Three developmental traits were investigated: the developmental mode of trunk segmentation, the average per-molt growth rate, and the conformity to a constant per-molt growth rate (Dyar's rule), for which an original metric was devised. Growth rates are within the normal range with respect to other arthropods and show overall conformity to Dyar's rule. Randomization tests indicate statistically significant phylogenetic signal for growth in early juveniles but not in later stages. Among five evolutionary models fit via maximum likelihood, one in which growth rates vary independently among species, analogous to Brownian motion on a star phylogeny, is the best supported in all ontogenetic stages, although a model with a single, stationary peak to which growth rates are attracted also garners nontrivial support. These results are not consistent with unbounded, Brownian-motion-like evolutionary dynamics, but instead suggest the influence of an adaptive zone. Our results suggest that developmental traits in trilobites were relatively labile during evolutionary history.

KEY WORDS: Evolutionary trends, fossil arthropods, growth, molt cycle, ontogeny, phylogenetic signal.

Ontogenetic series of extinct species add to the knowledge of developmental diversity derived from studies of living organisms, and can provide evidence for the phylogenetically basal developmental character states of major clades. They serve a critical role in defining the polarity of evolutionary change in development by revealing how ontogeny has itself evolved (e.g., Waloszek and Maas 2005; Long et al. 2009; Harvey et al. 2010). Moreover, the study of fossilized ontogenies can also provide insights into how developmental processes have affected evolution. Evolvability and evolutionary patterns can be variably influenced by the ways in which different developmental processes are interrelated, which govern the magnitude and direction of phenotypic variation available to selection (Müller 2007).

Despite the potential of a developmental approach to phenotypic evolution in extinct clades, the vagaries of preservation have resulted in a fossil record of ontogeny that is of variable quality. Preservational factors hinder our ability to draw general conclusions about the evolution of development within extinct clades. However, for certain groups a relatively rich, if patchy, record of ontogenetic series is currently available (e.g., Smith 2005). This is the case for a major clade of extinct arthropods, the Trilobita. Early ontogenetic onset of biomineralization in this clade has resulted in a developmental record that is among the most comprehensive for any extinct group (Hughes 2007).

Due to their basal phylogenetic position and geological age, trilobites putatively exhibit traits in their ancestral state for the Arthropoda, and trilobite ontogeny may thus shed light on

ancestral features of arthropod development (Hughes et al. 2006). Moreover, trilobite postembryonic development is characterized by an early phase of trunk segment addition (hemianamorphic development) that is also typical of basal clades in all major extant arthropod lineages (Fusco 2005), possibly representing the primitive condition for all arthropods (Hughes et al. 2006).

Here we analyze growth patterns in a sample for which quantitative data on segmentation and growth increments between putative successive instars are available, and perform a phylogeny-based analysis of trilobite postembryonic development. This may provide some indication of the evolution of early euarthropod body patterning which, along with consideration of other factors (e.g., ecological or environmental), may contribute to understanding the evolution of this clade.

Outline of Trilobite Development

Early onset of biomineralization, presumably shortly after hatching, yields an extended series of gradually changing instars (developmental stages comprised between two consecutive molts). The standard trilobite life-history phases are based on the development of articulating joints between segments (see Hughes et al. 2006). An anterior set of conjoined segments comprised the cephalon, thought to have had a stable complement of segments throughout ontogeny. The trunk region lay posterior to the cephalon and changed dynamically during ontogeny in both the number of segments expressed and in the number of articulating joints between segments. The initial (controversial) biomineralized ontogenetic phase, the *phaselus* period, is known in few taxa, and the earliest widely recognized phase of trilobite ontogeny is the *protaspid* period, during which all body segments (both cephalic and trunk) formed an undivided shield (Chatterton and Speyer 1997; Fig. 1). This period typically embraced a small number of instars. Later instars were characterized by the appearance of a series of articulations, the first of which occurred at the cephalon-trunk boundary.

The appearance of cephalic-trunk articulation marked entry into the *meraspid* period, which divided the shield into two components, the cephalon and a set of conjoined trunk segments called the pygidium. During subsequent meraspid molts, new articulations developed sequentially between anterior trunk segments, resulting in an anterior set of articulating trunk segments, called the thorax, in front of the pygidium (Fig. 1). Throughout juvenile growth, new trunk segments appeared sequentially in a subterminal zone within the pygidium, and the expression of new segments near the rear of the pygidium and release of older segments at the anterior of the pygidium maintained a rough balance. The meraspid period was divided into a series of "meraspid degrees," defined by the number of freely articulating segments within the thoracic region. Meraspid degrees did not necessarily correspond to meraspid instars, as cases of irregular release are known (Chatterton and Speyer 1997). The rate at which segments were released into the thorax relative to the rate at which segments were expressed in the subterminal growth zone determined the number of segments allocated to the meraspid pygidium, and varied among species. Progressive release of trunk segments into the thorax continued until the individual entered the final, *holaspid* period of development, characterized by a stable number of thoracic segments.

Trilobite ontogeny can also be subdivided into an *anamorphic* phase, during which new trunk segments appeared at the rear of the trunk, and a subsequent *epimorphic* phase, during which the number of trunk segments remained constant (*hemi-anamorphic* development, Minelli et al. 2003). Transition to the epimorphic phase could precede, coincide with, or follow onset of the holaspid period. Accordingly, with respect to the holaspid/epimorphic transition three different developmental modes have been recognized among trilobites (see below).

Exoskeletal growth in arthropods occurs in a stepwise manner, with postembryonic development paced by the molt cycle. A constant rate of per-molt size increase, the so-called Dyar's rule
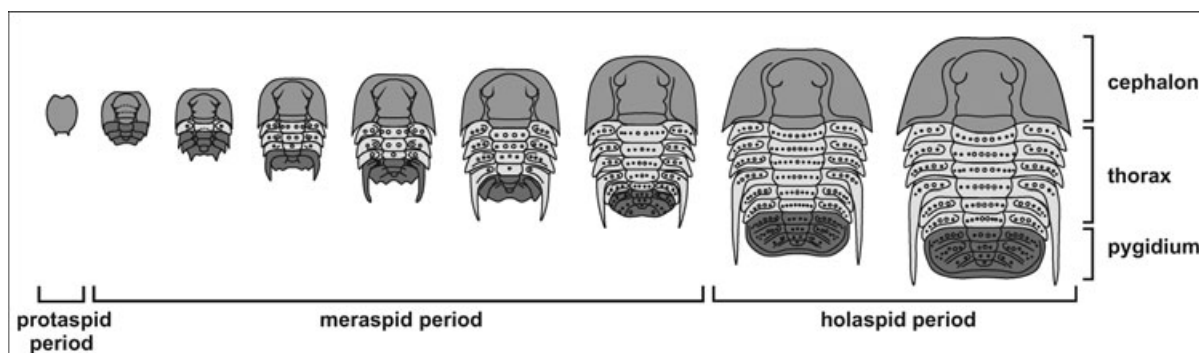

Figure 1. Schematic representation of trilobite postembryonic development with focus on body segmentation and regionalization (tagmosis), based on the ontogeny of *Shumardia (Conophrys) salopiensis* (Stubblefield 1926; Waisfeld et al., 2001). Several variants to this ontogenetic pattern are known among Trilobita (see text).

(Dyar 1890), is considered the "null model" for arthropod growth, and conformity to Dyar's rule has been reported for portions of the ontogeny of various trilobites (Chatterton and Speyer 1997; Fusco et al. 2004). However, due to ontogenetic allometry, different characters may exhibit different growth rates within the same species and ontogenetic phase.

Materials and Methods
DATASET CONSTRUCTION
Quantitative data on growth increments between putative successive instars have been published for over 75 trilobite species, from strata ranging from early Cambrian ($\sim$516 Ma) to Carboniferous in age ($\sim$322 Ma). These instar series include representatives of all trilobite life-history stages, and span a broad range of environmental settings. Our dataset is based on published records and our own analyses and includes all papers providing relevant information known to us published up to March 2009 (Tables S1and S2). Values for linear size traits were extracted either directly from published data tables, via the digitization of published graphs, or from our own analyses. For each species, additional information was recorded on taxonomy, stratigraphic age, developmental mode, and paleoenvironmental setting (see below).

We gathered data for all cases in which putative sequential instars were reported but, in our opinion, some lacked cogent justification due to small sample size and/or weak criteria for instar assignment (see Tables S1and S2). For the comparative analyses presented herein, we employed an inclusive approach and, after culling, the final dataset includes 60 species, ranging in age from the early Cambrian to the late Devonian ($\sim$360 Ma, see Table S1).

SIZE TRAITS THROUGH ONTOGENY
We recorded nine linear measurements. Values consisted of a series of static morphometric data, each relating to a different instar and a different set of individuals. For most species, instar assignment involved a criterion independent of size, such as the number of trunk segments (cross-sectional sensu Cock 1966), whereas for four species instar assignment was based solely on specimen size clustering (mixed cross-sectional sensu Cock 1966). All metric measures were transformed into their natural logarithms prior to statistical treatment, and are here referred to as log-size traits (sensu Mosimann 1970).

The nine traits are *Body Length*, *Body Width*, and a compound measure of overall *Body Size* (*BoL*, *BoW*, and *BoS*, respectively), and analogously for the cephalon (*CeL*, *CeW*, and *CeS*) and pygidium (*PyL*, *PyW*, and *PyS*). For each specimen, the compound measures were calculated as the arithmetic mean of the other two log-size traits (this is equivalent to the logarithm of the geometric

mean of the original, untransformed size traits). In most analyses, when only one measure was available for each specimen of that species, we considered either length, width, or the mean of length and width measured on different specimens as a proxy for the compound measure (see Table S1).

Separate cephalic and pygidial measures did not apply to phaselus and protaspid stages, whereas whole-body measures have not been considered for meraspid and holaspid stages, as these are not generally available (complete meraspid or holaspid exoskeletons are very rare or absent for many of the species).

ADDITIONAL MORPHOLOGICAL TRAITS
The values of these morphological traits refer to the value recorded at a mature, holaspid stage.

Size CLass (*SCL*) is a ranked categorical variable with four classes that designate the approximate maximum body length observed at maturity: 1 = up to about 1 cm, 2 = from about 1 cm to about 5 cm, 3 = from about 5 cm to about 10 cm, 4 = larger than 10 cm.

The other three traits in this group are the *Number of THoracic segments* (*NTH*), the *Number of TRunk segments* (*NTR*) (thorax plus pygidium), and their ratio (*NTH/NTR*). These data are available for 54 of 60 species in the dataset. For 21 species, *NTH* and *NTR* were inferred from close relatives (see Table S1). *NTH* and *NTR* present intraspecific variation in *Aulacopleura konincki*, from 18 to 22 and from 21 to 27, respectively. We present calculations using the median value of *NTH* = 20 and *NTR* = 24, but using extreme values (*NTH* = 18 and *NTR* = 21, *NTH* = 22 and *NTR* = 27) does not alter the results.

DEVELOPMENTAL TRAITS
These morphological data and other information on segment development have allowed us to define three developmental traits, which consider the average per-molt growth rate, the ontogenetic variation of this growth rate, and the mode of trunk segmentation.

Average per-molt Growth Increment (*AGI*) is a continuous variable, the value of which depends on the combined dynamics of the growth process and the molt cycle. Log-transformation of a size trait converts the geometric progression expected under the hypothesis of growth at a constant rate (constant size ratio between contiguous instars, or Dyar's rule) into a more statistically tractable version of the same, that is, a linear progression that is characterized by a specific, constant per-molt growth increment (constant log-size difference between contiguous instars). As conformity to a growth progression at a constant rate cannot be assumed a priori for all species (see below), a linear regression cannot be adopted as a general model for estimating average growth increment of log-size traits in trilobite ontogeny. *AGI* is thus calculated as the average log-size increment between pairs
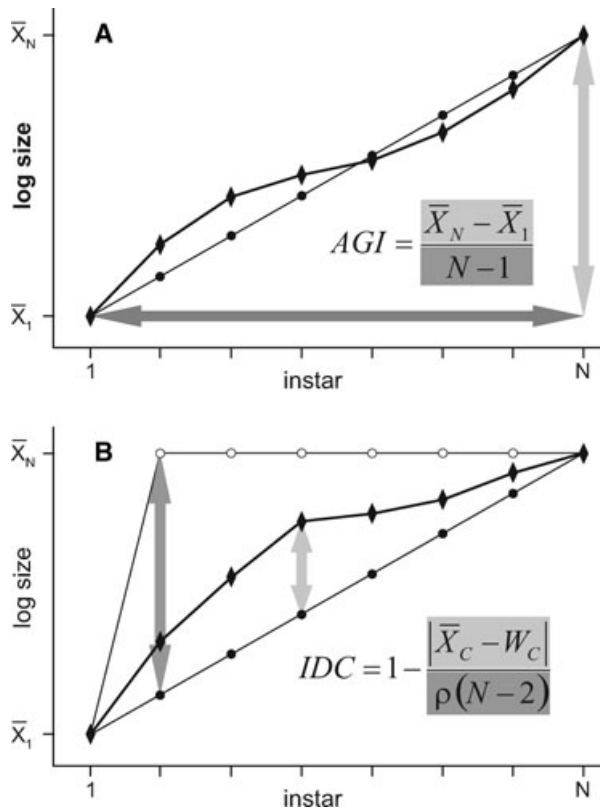
Figure 2. Geometric significance of the two developmental traits average per-molt growth increment (*AGI*, panel A) and index of conformity to Dyar's rule (*IDC*, panel B), as these are calculated on the basis of the ontogenetic progression of a log-size trait across *N* instars (diamonds). Small black dots show the growth progression at a constant rate for the same final size growth. In panel B, small empty circles indicate a growth progression where the final size is obtained in single molt (in the case depicted, the first one) that represent the maximum discrepancy from a growth progression at a constant rate. Light and dark gray arrows, respectively, indicate numerator and denominator in the formulae.

of contiguous instars in the ontogenetic series. This simplifies to the ratio between the total growth increment and the number of molts, or

$$AGI = \frac{\bar{X}_N - \bar{X}_1}{N - 1},$$

where $\bar{X}_N$ and $\bar{X}_1$ are the mean log-size of the last (*N*th) and the first instars of the series, respectively, and *N* is the number of instars (Fig. 2A). The average per-molt growth rate (*AGR*) of the original, untransformed size trait can be simply calculated as the anti-logarithm of *AGI* estimate of the corresponding log-size trait. For details of the estimation of *AGI* central value and standard error, see Appendix S1.

Index of conformity to Dyar's rule (*IDC*) is a continuous metric that quantifies the fit of the ontogeny to growth progression at a constant rate (Dyar's rule). Because ontogenetic series differ

in the number of instars per series (from 2 to 13) and, within a series, different instars are generally represented by a different number of specimens (in the whole dataset, from 1 to 55), it is not possible to distinguish between structural deviation from a constant growth model and sampling error with a comparable level of precision across the whole dataset. Hence, for evaluating the conformity to Dyar's rule, we adopted a "coarse-grained" quantitative approach. We devised a new metric that, for a given ontogeny, evaluates the extent to which instar average log-size, calculated on the basis of a constant growth model, is effective at predicting observed instar average size. The two extreme instars are excluded, as these are used to calculate *AGI*. *IDC* is thus calculated as

$$IDC = 1 - \frac{\left| \bar{X}_C - W_C \right|}{\rho (N - 2)},$$

where $\bar{X}_C$ is the observed mean log-size of the instar (*C*th) that presents the maximum deviation from the corresponding expected mean log-size (W_C) under a constant growth, ρ is the calculated average growth increment (*AGI*), and *N* is the number of instars. The denominator in the right-hand term, $\rho(N - 2)$, represents the maximum possible deviation from constant growth (Fig. 2B). *IDC* applies to growth progression developed on at least three instars ($N > 2$). It varies between 0 (maximal divergence from Dyar's rule, i.e., totality of growth achieved either at the first or at the last molt) and 1 (perfectly constant growth rate). The metrics can give negative (i.e., nonsensical) results in the case of ontogenetic size decrease. *IDC* calculation can be applied to a broad range of data structures, as frequently encountered in meta-analyses of wide taxon-coverage datasets. For details on the estimation of *IDC* central value and confidence interval, see Appendix S1.

Developmental Mode (*DM*) describes the development of trunk segmentation. It combines aspects of ontogenetic change in trunk segment articulation with the scheduling of trunk segment production (see above). *DM* has three values: *protarthrous*, in which the onset of the holaspid period preceded onset of the epimorphic phase, *synarthromeric*, in case of synchronous onset of both holaspid period and epimorphic phase, and *protomeric*, when onset of the epimorphic phase preceded the onset of the holaspid period (Hughes et al. 2006, Fig. S1). For phylogenetic analyses, *DM* has been considered as a semi-quantitative variable (with values scored 0, 1, and 2). Of 60 species in the final dataset, 39 (65%) yielded ontogenetic sequences that permitted assessment of developmental mode.

PALEOENVIRONMENTAL INDICATORS
We have explored whether trilobite developmental traits can be related to independent, physical indicators of their paleoenvironment. The dataset includes geological information about

paleoenvironmental setting and a qualitative estimate of available oxygen level at the seafloor. Our dataset encompasses a diversity of trilobite morphotypes; almost all of the instars included lived benthically (only three species included data from putatively pelagic protaspid stages). Given the small sample size available for most of the analyses we attempted, we extracted two, two-value qualitative variables from this information.

Water Depth (*WD*) is an indicator that scores either *shallow* or *deep*. Paleoenvironmental settings considered to be "shallow" include the carbonate platform and inner shelf, whereas those that were "deep" include back arc basins, slope, and outer shelf settings (see Table S1).

Oxygen level (*OL*) is an indicator that scores either *normal* or *reduced*. The degree of confidence in the assessment of oxygen availability was not very high for 25% of the species (see Table S1), but in none of these cases was the degree of uncertainty enough to recommend species exclusion. Thus, all species were placed in one of the two categories based on our best estimate.

For phylogenetic statistical analyses (see below), both *WD* and *OL* have been considered as semi-quantitative traits (with values scored 0 and 1). There was a relationship between water depth and levels of inferred oxygen availability: deeper water settings were more commonly oxygen depleted than shallow ones. However, during the Paleozoic this association was quite commonly decoupled during intervals in which wide portions of the shallow shelf sea became dysoxic, as indicated by sulphur mineralogy and sedimentary fabric (Peters 2007; Gill et al. 2011).

PHYLOGENETIC FRAMEWORK (TREE ASSEMBLY)
Topology

Taxa included in this analysis are a haphazard sample of the approximately 22,000 trilobite species currently recognized to be valid. Taxon selection was determined by developmental data availability alone, and thus our sampling is uneven with respect to both the phylogenetic and temporal diversity of the clade. Although most of the major trilobite clades are represented (except the recently proposed Order Harpetida, which comprises a small number of species [Ebach and McNamara 2002]), coverage within clades is sporadic and some clades, such as Asaphida, only include members whose form is markedly atypical of the clade as whole. Nevertheless, species analyzed included at least two representatives of all but two of the currently recognized orders, and with many of the suborders represented by several species. This haphazard sampling, coupled with incomplete character data for many of the species in the dataset, precluded formal analyses to infer the phylogenetic relationships of the species in the dataset. Accordingly, we have constructed a phylogenetic scheme that is collated from recent views of trilobite higher level systematics (e.g., Fortey 1990, 2001; Lieberman and Karim 2010) and phylogenetic analysis of particular clades where available (Fig. 3,

Appendix S2). Where alternative topologies have been proposed, we have preferred those with better taxon sampling and topology support. Where no phylogenetic analysis has been published, ingroup relationships have been inferred based on consultation with clade specialists. Our diagram expresses the observation that the major trilobite classes, many of which have been recognized for over 100 years, can in most cases be defined as monophyletic entities (clades), although some such as "Ptychopariida" are likely paraphyletic at best. However, the relationships among the classes are poorly known, and the degree of resolution shown is evidently unsatisfactory (see Appendix S2).

Node dating

The stratigraphic age of each terminal taxon was estimated based on the biostratigraphic information provided in the original publications or in references therein (see Appendix S2).

TREE-BASED ANALYSES
Phylogenetic signal

Phylogenetic signal is the tendency for related organisms to resemble each other, and its presence has implications for understanding how traits evolve, and how data are best analyzed in the context of a phylogeny (Blomberg and Garland 2002; Blomberg et al. 2003; but see Revell et al. 2008). Phylogenetic signal was ascertained using a randomization test for the mean-squared error (MSE) as described in Blomberg et al. (2003, Matlab program PHYSIG_LL.m, see Appendix S3 for the ASCII format data file used for these analyses). We also calculated their *K*-statistic as a measure of the amount of signal.

Evolutionary model fitting

To understand better the evolutionary dynamics of growth rate, we fit a set of evolutionary models to the *AGI* values for the protaspid, meraspid cephalon, and meraspid pygidium datasets. We considered five distinct evolutionary dynamics: Brownian motion (BM), accelerating/decelerating evolution, single stationary peak, uncorrelated white noise, and constant trend models.

Under BM, evolutionary changes are independent, nondirectional, and occur at a constant instantaneous rate, β, throughout the phylogeny. The accelerating/decelerating evolution model (ACDC, Blomberg et al. 2003; also known as early burst, Harmon et al. 2010) is similar, except that the Brownian rate parameter decreases or increases exponentially over time as $\beta(t) = \beta_0 \exp(rt)$, where t is time, β_0 is the rate at the root of the tree, and r modulates the change in the BM rate. When r is negative, traits evolve rapidly at first, but slow over time, as in some notions of adaptive radiation (Harmon et al. 2010). Positive r values indicate accelerating evolutionary rates, as might occur after an innovation or mass extinction (Blomberg et al. 2003).
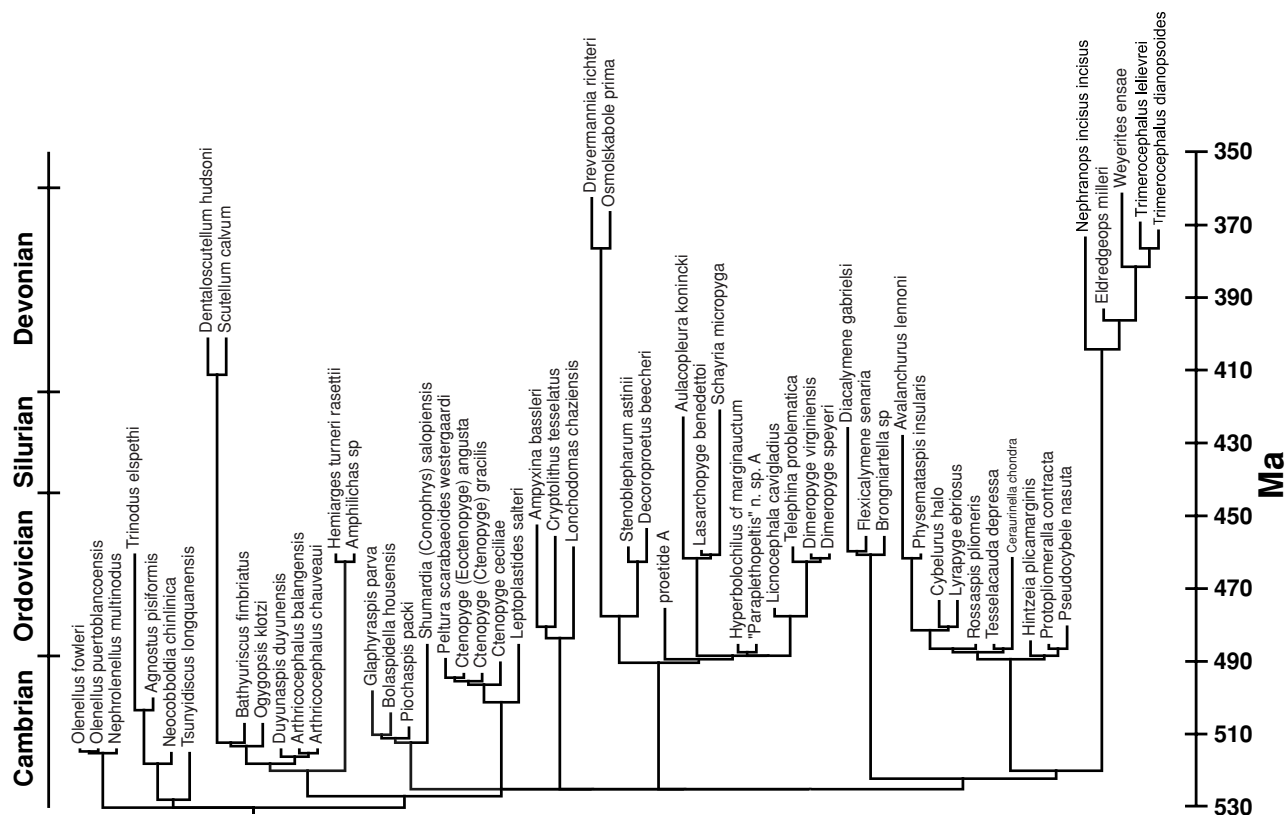
Figure 3. A phylogeny of the 60 trilobite species included in our dataset for which quantitative data on ontogenetic growth progression are available. Details of the construction of this diagram are given in Appendix S2.

The single stationary peak model is an Ornstein–Uhlenbeck (OU) process in which a trait value acts as an evolutionary attractor. In macroevolutionary studies, this attractor has been interpreted as the phenotypic center of an adaptive zone (Felsenstein 1988; Garland et al. 1993; Hansen 1997; Butler and King 2004). In addition to a rate parameter, this model has a parameter α that measures the strength of attraction to the optimum (see Blomberg et al. 2003 and Lavin et al. 2008 for an alternative parameterization of an OU process). When attraction to the optimum is absent (α = 0), this process reduces to BM. With increasing values of α, the influence of the optimum grows more pervasive; at very high values, taxa are pulled so strongly to the optimum that the signature of history is erased (Felsenstein 1988; Hansen 1997). The strength of α can be appreciated by considering the phylogenetic half-life, the expected time to reduce by half a taxon's distance to the optimum, computed as $t_{1/2} = \ln(2)/\alpha$ (Hansen 1997).

The fourth model can be thought of as an extreme version of an OU process in which the strength of attraction to the optimum is infinitely strong. The resulting trait will be independently distributed among species, equivalent to BM on an unstructured (star) phylogeny (BM-star). Because species values are independent, this model predicts that traits in sister taxa will be no more

similar than in distant relatives, and thus bear no phylogenetic signal.

The final model considers BM with a uniform trend in *AGI* values over time resulting from a constant bias in the direction of evolutionary change (Pagel 2002; Hunt and Carrano 2010), analogous to a phylogenetic regression that includes time since the root as a predictor of taxon values. In addition to the BM rate, this model also has a parameter, μ, indicating the directional bias in evolution, equivalent to the slope of trait values with respect to time.

Models were fit via maximum likelihood using the function *fitContinuous* in the R package geiger (Harmon et al. 2009) using the *model* argument set to "BM," "EB," "OU," "white," and "trend," respectively. The standard errors for *AGI* (see Appendix) were incorporated into the expected variance of trait values (see Ives et al. 2007) using the *meserr* argument to *fitContinuous*. BM and BM-star (obtained from the "white" argument) are the simplest of the candidate models, with only one additional parameter each beyond the ancestral trait value at the root of the tree (the estimated value at the root is a parameter in all the models). Each of the remaining models has three parameters. Small-sample Akaike information criterion scores (AIC$_C$)

were used to balance log-likelihoods and model complexity, and for convenience, these were converted to Akaike weights that represent the proportional support received by candidate models (Burnham and Anderson 2010). Because BM is nested within all the three-parameter models, we also present ln maximum likelihood-ratio tests for these models against the null model of BM.

Initial results suggested that phylogenetic signal for *AGI* was modest to absent (see below), and yet the trend model above has a Brownian-motion like dynamic and so it assumes substantial phylogenetic signal. Therefore, to test more fully the suggestion that *AGI* values trend upward over time (Chatterton et al. 1990, p. 260), we performed additional analyses of trends comparing phylogenetic generalized least squares (PGLS) and ordinary least squares (OLS) regressions of *AGI* values against age (time since the root). In the absence of phylogenetic signal, the OLS regression is a more appropriate assessment of directional change in trait evolution.

Relation of developmental traits with paleoenvironmental indicators

Regression analysis was used for testing the association between developmental traits and paleoenvironmental indicators. Both PGLS and OLS regressions were computed using the Matlab program REGRESSION version 2.m (Lavin et al. 2008, see Appendix S3 for the ASCII format data file used for these analyses).

REMARKS ON SAMPLING

A considerable amount of missing data characterizes our dataset (Tables S1 and S2). Even excluding the poorly known phaselus phase, the theoretical number of records for *AGI* calculation for 60 species is 900 (60 times 15, the number of possible measures, 3 for protaspids + 6 for meraspids + 6 for holaspids), but available records span only 205 cases (23%). The number of *IDC* estimates is even smaller, 117 (13%), principally because *IDC* cannot be calculated for two-instar ontogenies, which are very common in the protaspid dataset. *AGI* missing data are unevenly distributed among the three postphaselus developmental phases: there are 93 available records for 180 possible estimates (52%) for protaspids, 92 of 360 (26%) for meraspids, and only 20 of 360 (6%) for holaspids. Completeness is higher when considering the proportion of species for which growth data are available for any dimension (length, widths, or both) for protaspids (38 of 60, 63%) and meraspids (43 of 120, 36%).

Results

DESCRIPTIVE AND CORRELATION STATISTICS OF DEVELOPMENTAL TRAITS

AGI and AGR

Although all computations and statistics have been carried out on log-size traits, producing *AGI* estimates, tabular results are presented as *AGR* values as these provide a more intuitive indication of ontogenetic growth increments (Table 1). *AGR* values vary from 1.00, that denotes no growth (values not significantly larger than 1.0 are recorded for some protaspid and meraspid pygidial measures), to 2.22 (more than a size doubling per molt, more frequently approached earlier in ontogeny, in the phaselus and protaspid phases). Examination of the ontogenetic series for individual species indicated little allometry between length and width measurements of the same body region (either the cephalon or the pygidium, results not shown), consistent with previous studies (e.g., Fortey and Morris 1978 Fig. 2B; Clarkson et al. 2003 text-Fig. 6; Lerosey-Aubril and Feist 2005 Fig. 5). Inspection of Table 1 also suggests that the *AGI* values for length and width were generally quite similar, indicating minimal change in proportions along ontogeny. Allometry is a little more marked in the protaspid

Table 1. Summary statistics for the average per-molt growth rates (*AGR*, the anti-logarithm of *AGI*) in different developmental phases, body regions, and measures. The decimal figures can be read as the percentage per-molt growth increment (e.g., 1.72 = 72%). Here and in Table 2 the sample sizes of the compound size measures are lower than those presented in Tables 3–6 and Figures 4, 5, 7 because, to maximize taxon sampling, in those analyses species for which only a single measure was available the length or width value alone was used as the compound measure value (see Materials and Methods section and Table S1).

Phase/Region	Compound size			Length			Width		
	Median	Range	N	Median	Range	N	Median	Range	N
Phaselus body	1.72	1.63–1.80	2	1.83	1.56–2.16	2	1.61	1.51–1.72	2
Protaspid body	1.30	1.05–1.70	27	1.32	1.04–1.77	35	1.25	1.00–2.21	31
Meraspid cephalon	1.18	1.09–1.35	10	1.16	1.09–1.38	18	1.23	1.12–1.83	18
Meraspid pygidium	1.15	1.03–1.33	12	1.14	1.01–1.45	19	1.15	1.06–1.87	15
Holalspid cephalon	1.23	1.22–1.25	2	1.26	1.20–1.84	4	1.25	1.10–1.29	5
Holaspid pygidium	1.23	1.22–1.24	2	1.25	1.17–2.22	3	1.25	1.22–1.33	4

period (*AGI* for *BoL* tends to be slightly larger than that for *BoW*), but this is due to the fact that the body measures available for the protaspid stage included the effect of the ontogenetic increase in the number of trunk segments (anamorphosis, see below).

Unfortunately, it is rare for the preserved ontogeny of a species to span both protaspid and meraspid stages, and so *AGI* values cannot be compared reliably within species. However, when *AGI* frequency distributions of width measures of the two developmental periods are compared across the pooled samples (to prevent the anamorphosis effect in the protaspids, see above), differences between protaspids and meraspids are not statistically significant (Wilcoxon test on medians between meraspid *CeW* and protaspid *BoW*, $P = 0.597$). In contrast, length *AGI* values are significantly higher in the protaspid than the meraspid stage (Wilcoxon test on medians between meraspid *CeL* and protaspid *BoL*, $P = 0.018$), and this is reflected in the different frequency distributions of the corresponding overall size measures (Fig. 4). In meraspids, the *AGI* for *CeS* and *PyS* are significantly related across species (Pearson product moment $r = 0.917$, $N = 12$, $P < 0.0001$).

We tested whether *AGI* could be predicted by a developmental mode. Only meraspid data have been analyzed, as most species with protaspid data present the same developmental mode (14 of 24 are protomeric, see next). In meraspids, there is no significant effect of the developmental mode on either *AGI* traits (both OLS and PGLS regressions, $P > 0.30$).

IDC

Conformity to Dyar's rule values varies in the range 0.07–1.00 (Table 2), but in 79% of the estimates it is larger that 0.80, with an overall median value of 0.89 ($N = 120$). In meraspids, *IDC* of the cephalon is significantly larger than that of the pygidium, indicating closer conformity to Dyar's rule in the head region (conventional Wilcoxon test on medians, $P = 0.014$, Fig. 5). In meraspids, there is no significant effect of the developmental mode on either *IDC* traits (both OLS and PGLS regressions, $P > 0.10$).
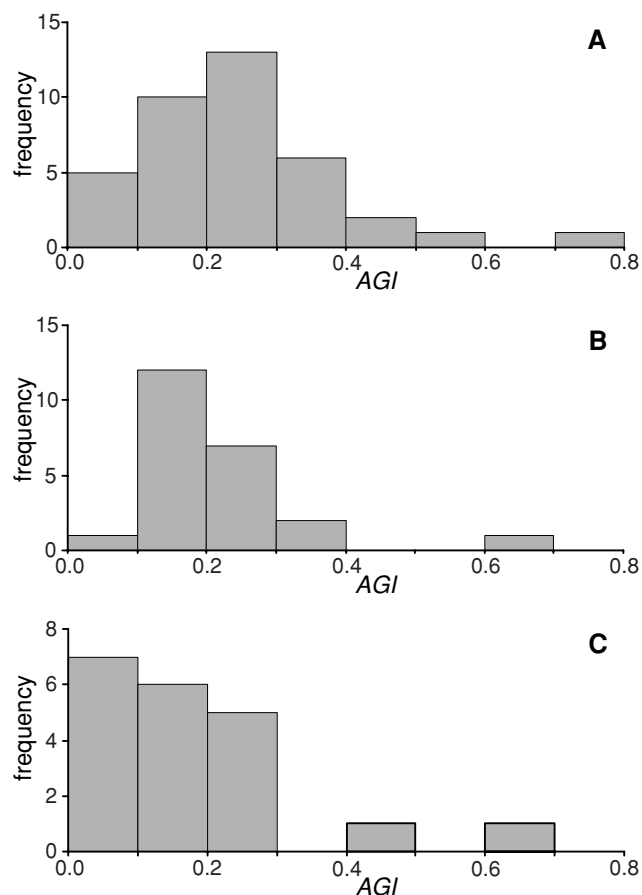

Figure 4. Frequency distribution of the average per-molt growth increment (*AGI*) for protaspid body size (*BoS*, *N* = 38, panel A), meraspid cephalon size (*CeS*, *N* = 23, panel B), and meraspid pygidium size (*PyS*, *N* = 20, panel C). Sample sizes are larger from those listed in Table 1 because here, to maximize taxon sampling, when only one measure was available for the species, either length or width was considered as a proxy for overall size (see section Materials and Methods).

DM

Developmental mode, assessed for 39 species of 60, shows a preponderance of protomeric species (24, 62%) in the dataset. The other two modes, synarthromeric and protarthrous, are

Table 2. Summary statistics for the index of conformity to Dyar's rule (*IDC*), that varies in the closed interval [0–1].

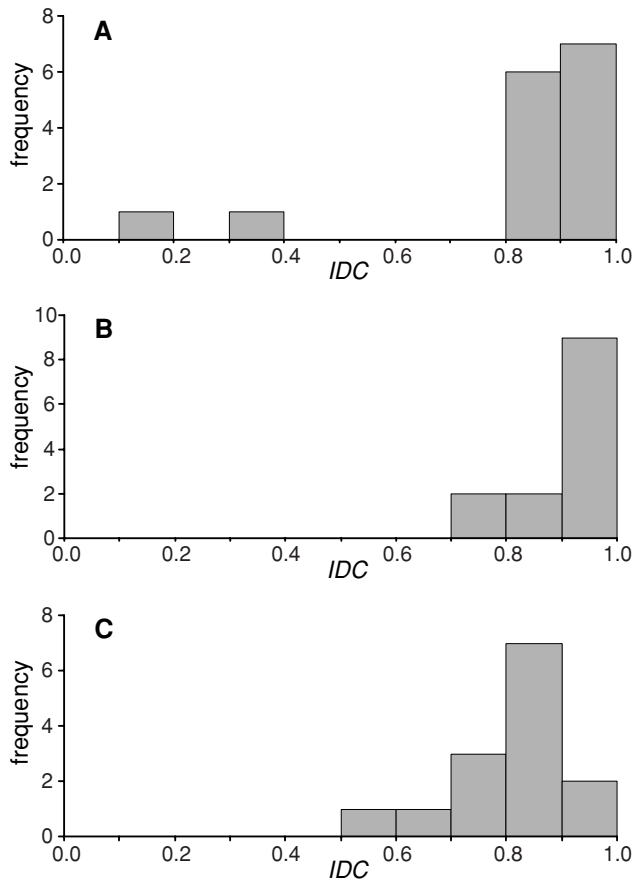| Phase/region	Compound size			Length			Width		
	Median	Range	N	Median	Range	N	Median	Range	N
Phaselus body	0.88		1	0.87		1	0.88		1
Protaspid body	0.90	0.18–1.00	15	0.89	0.24–0.96	14	0.92	0.07–1.00	15
Meraspid cephalon	0.94	0.78–1.00	9	0.93	0.88–0.98	10	0.92	0.59–0.99	11
Meraspid pygidium	0.88	0.61–0.96	12	0.79	0.54–0.98	13	0.89	0.65–0.98	11
Holalspid cephalon	0.93		1	0.94		1	0.83	0.75–0.92	2
Holaspid pygidium	0.99		1	0.98		1	0.99		1

Figure 5. Frequency distribution of the index of conformity to Dyar's rule (*IDC*) for protaspid body size (A, *N* = 15), meraspid cephalon size (B, *N* = 13) and meraspid pygidium size (C, *N* = 14). Sample sizes are different from those listed in Table 2 because here, to maximize taxon sampling, when only one measure was available for the species, either length or width was considered as a proxy for overall size (see section Materials and Methods).

represented by eight and seven species each, respectively (20% and 18%).

PHYLOGENETIC SIGNAL

For the continuous developmental traits, phylogenetic signal was tested in only three cases, all with respect to *AGI*, because other traits/cases lack sufficient sample size (Table 3). The randomization test indicates significant phylogenetic signal ($P = 0.006$, $K = 0.563$) for protaspid body size (*BoS*, Fig. 6) but not for meraspid cephalon size (*CeS*) or meraspid pygidium size (*PyS*) (Table 3). Developmental mode also shows significant phylogenetic signal (randomization $P = 0.041$), although not as strong ($K = 0.299$) as that for protaspid body size.

For comparison to the developmental traits, we also tested for phylogenetic signal in six other traits, four holaspid characters (size class (*SCL*), number of thoracic segments (*NTH*), number of trunk segments (*NTR*) and *NTH*/*NTR* ratio), and the two pa-

leoenvironmental indicators (water depth (*WD*) and oxygen level (*OL*)) (Table 3). The randomization test indicates low but statistically significant phylogenetic signal for size class ($P = 0.006$, $K = 0.182$). Likewise the number of thoracic segments, the number of trunk segments, and their ratio all show low but statistically significant phylogenetic signal (Table 3). Interestingly, in spite of the crude nature of the data for water depth and habitat oxygenation (both scored as 0–1 traits), both show phylogenetic signal (both $P < 0.001$, $K = 0.642$ and 0.485, respectively).

Note that in all cases shown in Table 3, the likelihood of the star is actually higher than that for the specified phylogenetic tree, which would suggest that the traits do not exhibit phylogenetic signal. This apparent discrepancy versus the significant randomization tests for phylogenetic signal can be explained by at least two, not-mutually exclusive possibilities. First, comparing likelihoods is not equivalent to testing a null hypothesis of no phylogenetic signal. In particular, model fitting can be sensitive to local departures from the assumed model. For example, although many closely related pairs of species (i.e., those connected by short branch lengths) have similar protaspid growth increments (e.g., *Amphilichas* sp. [Ax] and *Hemiarges turneri rasettii* [Ht], *Hyperbolochilus* cf. *marginauctum* [Hm] and "*Paraplethopeltis*" n. sp. A [Px], *Protopliomerella contracta* [Pc] and *Pseudocybele nasuta* [Pn]; see Fig. 7A), one pair of closely related species, *Arthricocephalus chauveaui* (Ac) and *Duyunaspis duyunensis* (Dd), is strongly dissimilar. This one anomalous pair will strongly reduce the likelihood of the BM model but have less effect on randomization tests, which are expected to be less sensitive to outliers. Of these two species, *A. chauveaui* (Ac) has an unusually large value, as compared with other species nearby in the phylogenetic tree (Fig. 6). Deleting this one tip changes the results as expected: the likelihood of the star tree becomes lower than that of the hierarchical tree (see Table 3). Second, the level of signal, as indicated by the K statistic, is not large for any trait (compare with values in Blomberg et al. 2003).

EVOLUTIONARY MODELS

In each *AGI* dataset, the BM-star model is best supported and the single peak OU receives secondary but nonnegligible support (Tables 4–5). For the full protaspid data, the support advantage of BM-star over OU is only modest (Akaike weights of 0.47 and 0.29, respectively). In all other datasets, BM-star is more decisively favored (Akaike weights > 0.70). This pattern of relative support is echoed in the parameter estimates for the OU models (Table 4). In the full protaspid dataset, the estimate of α is relatively low (0.078), and the resulting phylogenetic half-life is moderate—about nine million years (Table 4). In contrast, the remaining datasets yield much higher α values and corresponding half-lives that are extremely short (1–2 Ma) given the temporal scale of this phylogeny (Fig. 3). When α is quite high, the OU

Table 3. Statistics for randomization tests for significance of phylogenetic signal for nine measures as calculated with the Matlab program PHYSIG_LL.m (Blomberg et al. 2003). The phylogenetic tree is shown in Figure 3. Significant results for the randomization test of the mean squared error (MSE; lower values indicate better fit of tree to data) on the phylogenetic tree indicate the presence of phylogenetic signal. K-statistics indicate the amount of phylogenetic signal relative to a Brownian motion expectation of 1.00 (Blomberg et al. 2003). For analyses here and in Tables 4–6, growth (*AGI*) values were computed from lengths, widths, or their average if both were available, and thus the sample sizes do not match those in Table 1 (see text).

| Trait	Abbreviation	*N*	*K*	MSE	MSE star	*P* for signal	lnML	lnMLstar
protaspid *Body Size AGI*	*BoS*	38	0.563	0.0277	0.0225	0.006	14.6995	18.6471
protaspid *Body Size AGI* (Ac deleted)	*BoS*	37	0.623	0.0226	0.0227	0.003	18.1006	18.0403
protaspid *Body Size AGI* (Tl deleted)	*BoS*	37	0.210	0.0210	0.0149	0.008	19.4465	25.8196
protaspid *Body Size AGI* (Tl, Dr, Op deleted)	*BoS*	35	0.164	0.0208	0.0111	0.079	18.6276	29.6217
meraspid *Cephalon Size AGI*	*CeS*	23	0.125	0.0326	0.0124	0.370	7.2375	18.3244
meraspid *Cephalon Size AGI* (Tv deleted)	*CeS*	22	0.099	0.0189	0.0053	0.348	12.9320	27.0054
meraspid *Pygidium Size AGI*	*PyS*	20	0.100	0.0851	0.0201	0.842	−3.2233	11.1918
meraspid *Pygidium Size AGI* (Tv deleted)	*PyS*	19	0.135	0.0429	0.0096	0.812	3.4678	17.6771
Developmental Mode	*DM*	39	0.299	0.9479	0.6208	0.041	−53.7891	−45.5350
Size Class	*SCL*	60	0.182	1.1550	0.7850	0.006	−88.9437	−77.3818
Number of Thoracic Segments	*NTH*	54	0.294	56.208	52.288	0.042	−184.903	−182.951
Number of Trunk Segments	*NTR*	54	0.261	51.961	47.008	0.010	−182.781	−180.077
NTH/NTR		54	0.178	0.0447	0.0293	0.008	7.7943	19.1578
Water Depth	*WD*	60	0.715	0.1307	0.2542	<0.001	−23.5964	−43.5475
Oxygen Level	*OL*	60	0.491	0.1131	0.1989	<0.001	−19.2516	−36.1790
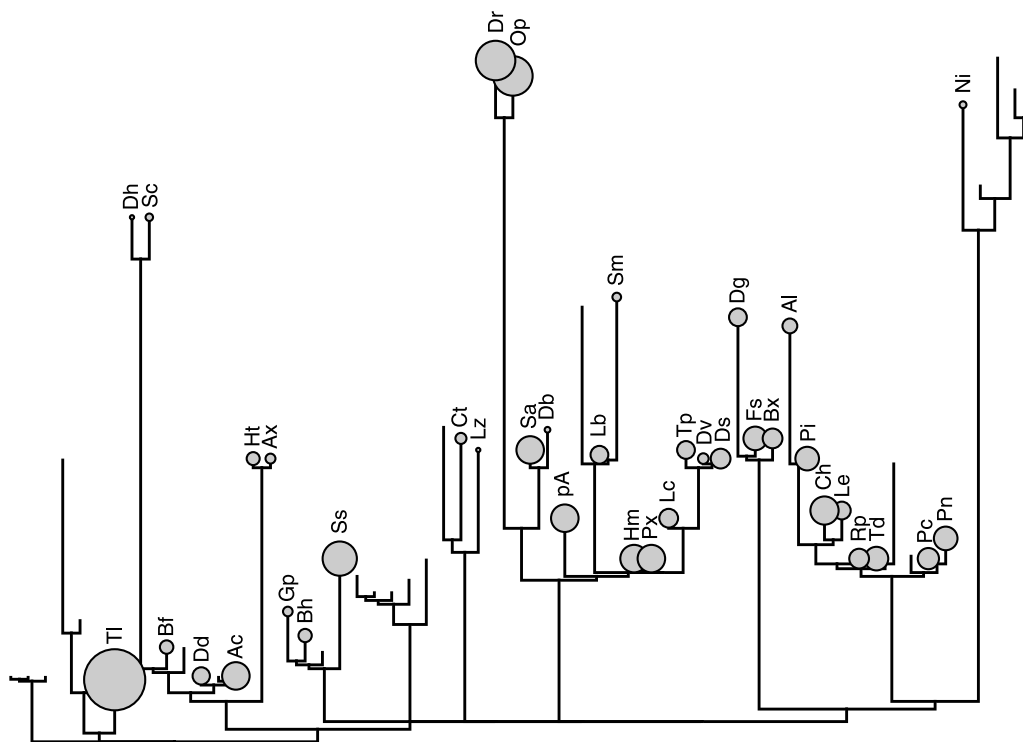
Figure 6. Protaspid body size *AGI* plotted onto the phylogenetic tree. Circle diameters are proportional to *AGI* values. Labels refer to species names, and branch lengths are proportional to absolute time (see Fig. 3). As shown in Table 3, this trait exhibits statistically significant phylogenetic signal.
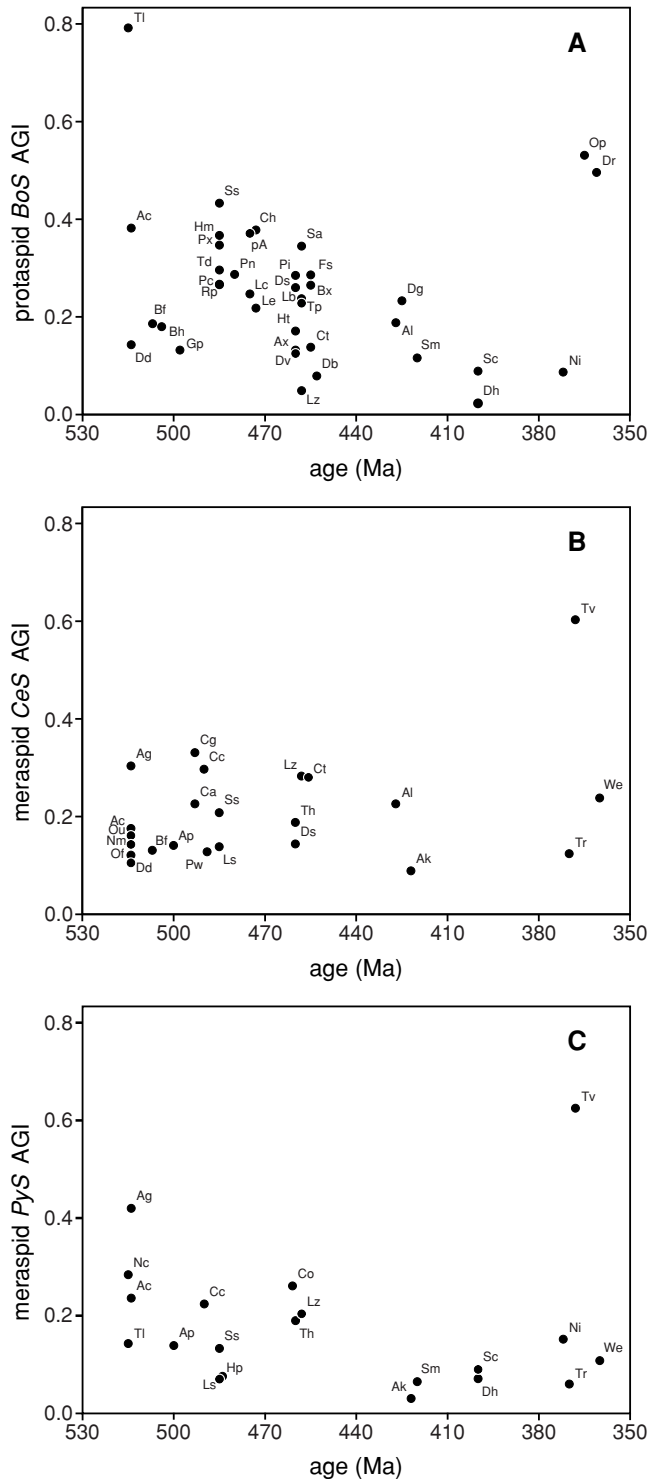
Figure 7. Scatter plots of developmental traits versus taxon age (Ma) for protaspid body size (A, *N* = 38), meraspid cephalon size (B, *N* = 23), and meraspid pygidium size (C, *N* = 20). The decreasing trends with time are nonsignificant. See Table 4 for statistical analyses and Table S1 for species labels.

process converges with BM-star, and these two models therefore have very similar ln maximum likelihoods (Table 4). Because the single peak OU has an extra parameter, AIC_C favors BM-star when the two models have nearly equal likelihoods (Table 5). These patterns of relative model fit and the parameter estimates for the OU model are consistent with the calculations of phylogenetic signal (Table 3): all approaches suggest greater presence of phylogenetic similarity in the protaspid than in the meraspid datasets.

The ACDC model receives moderate support for the full protaspid dataset, but this is largely driven by a single early-appearing taxon, *Tsunyidiscus longquanensis* (Tl) (Fig. 7A) that has unusually large growth between instars. Omitting this taxon, either singly (results not shown) or with two additional outlier taxa, results in much lower relative support for the ACDC model (Tables 4–5).

BM-like evolution along the tree shown in Figure 3 is poorly supported in all datasets (Tables 4–5); its Akaike weight is always negligible, and likelihood ratio tests consistently reject BM in favor of the single peak OU model (all $P < 0.005$, Table 5). BM with a trend offers only slight gains in likelihood over BM in exchange for its additional parameter (Table 4), and equivalent PGLS regressions do not find significant relationships between *AGI* and time (Table 6). There is some support for trends of decreasing *AGI* values over time when phylogeny is ignored, indicating a dynamic similar to BM-star but with a decreasing trend. But this result only holds when outlying taxa are removed, and even then only in two of the three *AGI* datasets (Table 6), so it should be treated with caution.

RELATION OF DEVELOPMENTAL TRAITS TO PALEOENVIRONMENTAL INDICATORS

There is no indication of an association between *DM* and *OL* (OLS regression, lnML = −44.468, $F = 2.08$, $P = 0.158$; PGLS regression, lnML = −53.185, $F = 1.17$, $P = 0.286$), but *DM* is related to *WD* (OLS regression, lnML = −41.379, $F = 8.79$, $P = 0.005$; PGLS regression, lnML = −52.038, $F = 3.48$, $P = 0.070$). This result may have biological significance but we cannot rule out preservational bias in shallow water (see Appendix S4): protomeric developmental mode is dominant in shallow water (protomeric:synarthromeric:protarthrous = 15:1:1, but in deep water the three developmental modes are equally represented = 9:7:6).

Relations with continuous developmental traits cannot be reliably tested in protaspids, as most of these species (26 of 38) are from the same paleoenvironment (carbonate platform, *OL* = *normal*, *WD* = *shallow*). For meraspids, none of the relationships with the two paleoenvironmental indicators are significant for either *AGI* or *IDC* in either OLS or PGLS regressions ($P > 0.50$, results not shown).

Table 4. Model fitting results for average per-molt growth increment (*AGI*). See text for parameter explanations. In parentheses after the OU α parameter is the equivalent phylogenetic half-life in Ma, which is a measure of how rapidly phylogenetic signal decays (see text). For each dataset, there were one to three outlying datapoints. Analyses were repeated after excluding these outliers. See Table 5 for comparisons of model fit statistics.

Trait	N	BM-star lnML	BM lnML	ACDC lnML	Single Peak OU lnML	Trend lnML	Trend parameter (μ)	ACDC parameter (r)	OU parameter (α)
Protaspid *AGI*	38	18.89	15.50	19.24	19.60	16.46	−0.0019	−0.021	0.078 (8.9)
Protaspid *AGI*	35	29.88	19.95	20.51	29.88	20.75	−0.0016	−0.010	57.3 (0.01)
Meraspid *Cephalon AGI*	23	18.32	7.33	7.33	18.77	7.34	0.0004	0	0.32 (2.19)
Meraspid *Cephalon AGI*	22	26.99	13.26	14.23	27.20	13.26	5.6e−06	−0.012	0.69 (1.01)
Meraspid *Pygidium AGI*	20	11.19	−3.16	−3.16	11.32	−3.06	−0.0011	0	0.55 (1.26)
Meraspid *Pygidium AGI*	19	17.68	3.74	8.97	18.12	4.08	−0.0013	−0.027	0.51 (1.36)

lnML = ln maximum likelihood; BM = Brownian motion; ACDC = accelerating or decelerating evolution; OU = Ornstein–Uhlenbeck; *N* = sample size.

Table 5. Comparing the fit among models presented in Table 4. After sample size (*N*), the next five columns are Akaike weights computed from AICc scores (best-supported model in bold). Last three columns report likelihood ratio (LR) tests. Given are the test statistic values, equal to twice the difference in log-likelihood between each model and BM, along with the relevant *P* value from a χ² distribution with one degree of freedom.

Trait	N	Akaike weights BM-star	BM	ACDC	Single Peak OU	Trend	LR test vs. BM Trend	ACDC	Single Peak OU
Protaspid *AGI*	38	**0.47**	0.02	0.21	0.29	0.01	1.92 P = 0.17	7.49* P = 0.006	8.22* P = 0.004
Protaspid *AGI*	35	**0.77**	0	0	0.23	0	1.59 P = 0.20	1.12 P = 0.29	19.85* P = 8.4e-6
Meraspid *Cephalon AGI*	23	**0.71**	0	0	0.29	0	0.028 P = 0.86	0.00 P = 1.0	22.89* P = 1.7e-6
Meraspid *Cephalon AGI*	22	**0.76**	0	0	0.24	0	0.00 P = 0.99	1.94 P = 0.16	27.87* P = 1.3e-7
Meraspid *Pygidium AGI*	20	**0.78**	0	0	0.22	0	0.20 P = 0.65	0.00 P = 1.0	28.95* P = 7.4e-8
Meraspid *Pygidium AGI*	19	**0.74**	0	0	0.26	0	0.68 P = 0.41	10.45* P = 0.001	28.76* P = 8.2e-8

Discussion

SOURCES OF ERROR

This study is a synthetic analysis of multiple data sources, and errors in parameter estimates in the original data cannot be accounted for easily. Failure to account for measurement error can have major effects on statistically analyses, including those that incorporate phylogenetic information (Ives et al. 2007; Felsenstein 2008). However, due to the disparity of methods and approaches used in the original works, it is improbable that our dataset contains systematic errors. This does not exclude the possibility of error in our individual estimates, in particular for species represented by small samples or short ontogenetic series.

Comparative analysis of trilobite growth patterns requires that the original, sequential instars have been recognized accu-

rately. Because of their molting habit, trilobite ontogenetic series are reconstructed by arranging individual specimens in sequences that show progressive changes in size and shape, and all such reconstructed series are hypotheses. Although we excluded cases in which previous claims of instars appeared spurious, it is possible that some of the growth parameter estimates included in our dataset are incorrect. However, the presence of a significant fraction of ontogenetic series of high quality (see Table S1), along with our restrictive criteria of taxon selection, should have kept the probability of incorrect estimates sufficiently low that descriptive statistics and hypothesis testing were not too adversely affected.

The phylogenetic scheme employed also imposes a limitation on this study, because it is partially unresolved and has nodes

Table 6. Statistics for phylogenetic generalized least squares (PGLS) regression and ordinary least squares (OLS) of developmental traits versus time (Ma from root of the tree) using real branch lengths. For each trait, tests were repeated excluding outliers. Removal of the outliers led to significant OLS regressions in two cases, but no significant PGLS regression was obtained for any trait. The phylogenetic tree is shown in Figure 3.

Trait	N	Model	lnML	Slope	F	P
Protaspid *Body Size AGI*	38	OLS	19.0780	−0.00057	0.83	0.368
		PGLS	15.5613	−0.00190	1.67	0.204
	35	OLS	34.5565	−0.00163	10.75	0.002
		PGLS	19.2570	−0.00162	1.21	0.279
Meraspid *Cephalon Size AGI*	23	OLS	19.9821	0.00083	3.26	0.085
		PGLS	7.2512	0.00040	0.03	0.865
	22	OLS	27.0171	0.00005	0.02	0.889
		PGLS	12.9320	0.00001	<0.001	>0.99
Meraspid *Pygidium Size AGI*	20	OLS	11.2852	−0.00025	0.17	0.685
		PGLS	−3.1236	−0.00109	0.18	0.676
	19	OLS	21.2265	−0.00102	7.70	0.013
		PGLS	3.7903	−0.00134	0.59	0.453

that are poorly supported (see Appendix S2). Its overall structure does, however, represent current consensus of trilobite relationships that is based on an explicitly phylogenetic approach (Fortey 1997, 2001). Furthermore, most of the major clades recognized have been accepted as natural groups for nearly 150 years (Salter 1864), and the in-group relationships shown are supported by phylogenetic analyses in many cases. With respect to branch lengths, as shown in Figure 3, stratigraphic ages of taxa can be considered as rather well defined.

DESCRIPTIVE ANALYSES

Growth rates within our sample are within the normal range with respect to other arthropods (e.g., Cole 1980; Rice 1968), and show a marked overall conformity to Dyar's rule (i.e., to a constant per-molt growth rate). This is partially due to the fact that we analyzed measures of size along the main axes of the body or body regions (cranidial length, pygidial width, etc.). Among living arthropods, more extreme growth values and more consistent deviations from a constant growth are recorded in more localized body structures, as for instance in the appendages (e.g., Klingenberg and Zimmermann 1992).

At face value, our results seem to imply that growth rates for protaspids exceeded those for meraspids, and this result is consistent with the conclusion of other studies of trilobites (e.g., Fortey and Morris 1978; Chatterton et al. 1990) and other arthropods (e.g., Hartnoll 1982). However, growth rates in protaspids and meraspids are not easily compared directly, because protaspid length-based growth estimates (body length) include the anamorphic addition of new trunk segments, whereas those of the meraspids (based on cephalon and pygidium length) do not account for the segments progressively allocated to the thorax. A

better comparison can be made between width-based estimates of protaspid and meraspid growth rates. As these do not differ significantly, we suggest that trilobite growth rates in the protaspid and meraspid periods were, in general, of comparable magnitude. This result is interesting in that it contrasts with the general impression that growth rates are higher earlier in ontogeny (Chatterton et al. 1990; Fortey and Morris 1978).

Conformity to constant growth rate for the cephalon was, in general, more marked than that for the pygidium. This is expected because the growth of the pygidium was commonly more complex than that of the cephalon. The complexity relates to the fact that premature pygidial growth included not only the growth of individual segments but also dynamic changes in the number and complement of segments that formed the structure.

In some asaphide trilobites a particular "metamorphic" molt shows an anomalous high degree of change in both morphology and size increment (Chatterton 1980; Speyer and Chatterton 1990). Under this hypothesis, conformity to Dyar's rule is expected to be relatively low for portions of ontogeny that include the metamorphosis, but no *IDC* values are available in our database for ontogenetic series that span the putative metamorphoses. However, relatively high growth increments (0.345, 0.496, and 0.531) were recorded between the two instars that demarcate metamorphosis in three species (the proetids *S. astinii*, *D. richteri*, and *O. prima*, respectively).

In meraspids, there is no significant effect of developmental mode on either *AGI* or *IDC* (see Results). This suggests that our inferences about the behavior of meraspid *AGI* or *IDC* are not biased by the fact that the protomeric condition is preponderant in our dataset (see below). More importantly, this result suggests that the mode of development, when considered in terms of the

combined effects of ontogenetic segment addition and development of segment articulation, is independent from the way in which size growth was paced by the molt cycle.

With regard to *DM*, in our sample all three developmental modes are equally represented in deeper water environments, but protomeric development overwhelmingly dominated in shallow water environments. However, the significant relationship between *DM* and *WD* might be taphonomic, rather than biological, in origin (see Appendix S4).

TREE-BASED ANALYSES

The success of the BM-star and single-peak OU models in accounting for the evolution of *AGI* is consistent with adaptive limits to growth increments between molts and inconsistent with unbounded, diffusion-like evolution. This interpretation with the OU model is self-evident, but for BM-star it may seem counterintuitive. When BM is better supported when fit to a star phylogeny than to the specified phylogeny, this means that phylogenetic relatedness poorly predicts trait similarity. One mechanism that may generate this pattern occurs when attraction to a macroevolutionary optimum is so strong that it erases the signal of history, and in fact, as one increases the attraction strength of the OU model it converges with the BM-star model. Alternatively, large measurement error in the tip data, the phylogenetic topology or the estimates of branch lengths could also produce this result (see also Blomberg et al. 2003, Ives et al. 2007).

Several explanations for specific values of per-molt growth rate have been offered for arthropods, spanning from "externalist" (e.g., ecological) to "internalist" (e.g., physiological) causes (see Fusco et al. 2004 and references therein). This issue cannot be easily investigated in fossils, but undoubtedly the strongly mineralized, virtually inextensible, exoskeleton of trilobites could pose strict limits to intermolt tissue growth (see Nijhout 1994), thus providing a plausible "internalist" explanation for why *AGI* variation was apparently restricted within the limits of a functional range.

Although the total range and variance of *AGI* values is similar among the different ontogenetic stages (Fig. 4; Levene's test for heterogeneity in variance among protaspid, meraspid cephalon, and meraspid pygidium datasets: $F = 0.536$, df $= 2, 75$, $P = 0.58$), protaspid *AGI* shows greater phylogenetic signal and a correspondingly longer phylogenetic half-life than meraspid *AGI*, either in the cephalon or in the pygidium (Table 3, 4). Thus, in the protaspid period, changes in *AGI* between ancestor and descendant tended to be modest compared to the total range of *AGI* values. This was not true in the meraspid stage, as many close relatives, such as *Trimerocephalus lelievrei* and *Trimerocephalus dianopsoides*, differ markedly from each other, resulting in rather little phylogenetic signal in growth increment in this stage.

In principle, these differences in evolutionary pattern between protaspid and meraspid *AGI*s could result from differences in the extent to which they are constrained by physiological or biomechanical factors, although hypotheses about such proximate mechanisms are exceedingly difficult to assess in extinct organisms with no obvious extant analogs. Furthermore, the same level of observed *AGI* variation in the two periods does not support the existence of different adaptive limits to growth rates in protaspids versus meraspids. As an alternative, the same developmental trait (*AGI*) could have exhibited different levels of integration with other traits (e.g., body size or intermolt duration) during the two ontogenetic periods, reflected in turn in a different pattern of change. For instance, it is possible that mature body size and the proportion of trunk segments allocated to the thorax, traits that certainly had adaptive value and exhibit a significant phylogenetic signal (Table 3), were more strictly dependent on meraspid growth pathways than protaspid growth, thus explaining the relatively higher "evolutionary dynamism" of the former with respect to latter. Besides, the fact that developmental mode, which exhibits phylogenetic signal, is not related to any growth-related developmental traits, suggests a certain degree of evolutionary independence among ontogenetic traits. However, the possibility that phylogenetic signal is reduced in the meraspid stage because of greater noise in growth estimates later in ontogeny cannot be completely dismissed (see also Blomberg et al. 2003; Ives et al. 2007).

The lack of relationship between meraspid *AGI* and paleoenvironment argues against simple environmental determination of the observed interspecific differences in growth patterns, at least at the coarse level at which environmental conditions (water depth, oxygen levels) can be characterized in the present study.

The generally poor support received by the trend model conflicts with Chatterton et al's. (1990) suggestion that growth increments tended to increase over trilobite evolution. Even ignoring this lack of model support, the trend parameter estimates and regression slopes are not consistent with this suggestion: they are either very close to zero (meraspid cephalon) or negative (protaspid and meraspid pygidium), suggesting decreasing growth increments over time (Tables 4, 6 and Fig. 7).

Overall, our results suggest that developmental traits in trilobites are relatively labile during evolutionary history (see also Webster and Zeldtich 2011). This lability may reflect a degree of evolutionary independence among developmental characters. For a given ontogenetic period, size and shape at any given instar depend on the combination of initial size and shape, the average per-molt growth rate (i.e., *AGI*), the distribution of growth during the period (partially accounted for by *IDC*) and the total number of instars in that period (data seldom available). All

these characters could change independently in evolution, so that the same phenotypic result (say, certain body proportions in the mature phase) could be obtained through different ontogenetic routes. Thus, variation in ontogenetic pathways is not necessary reflected in variation at certain time points in ontogeny.

CONCLUDING REMARKS

The present analysis cannot purport to be representative of the whole trilobite evolutionary history. Taxon sampling is limited and its composition entirely determined by data availability. An expanded dataset will permit a more hypothesis-driven approach. The difficulties in testing Chatterton's (1980) hypothesis of the association between metamorphosis and intermolt growth illustrates how many additional, high-quality ontogenetic series are needed before we can test satisfactorily multiple predictive hypotheses concerning the generality and taxonomic distribution of developmental phenomena.

More comprehensive studies of the ontogenies of the best-preserved species are necessary, in particular those that document multiple growth stages of the same species, those that incorporate some of the important taxa absent from our analysis (such as harpetids and nontrinucleoid "asaphids"), and also those that are able to examine multiple closely related taxa within individual clades.

Nevertheless, this study has delineated a "space of developmental pathways" for this group. An expanded database of trilobite ontogeny promises significant additional insights into the details of how developmental characters evolved in an ancient, diverse, and rapidly radiating arthropod clade, allowing the study of evolutionary change at different scales.

LITERATURE CITED

Blomberg, S. P., and T. Garland, Jr. 2002. Tempo and mode in evolution: phylogenetic inertia, adaptation and comparative methods. J. Evol. Biol. 10:899–910.

Blomberg, S. P., T. Garland, Jr., and A. R. Ives. 2003. Testing for phylogenetic signal in comparative data: behavioral traits are more labile. Evol. Dev. 57:717–745.

Burnham, K. P., and D. R. Anderson. 2010. Model selection and multimodel inference. Springer, New York.

Butler, M. A., and A. A. King. 2004. Phylogenetic comparative analysis: a modeling approach for adaptive evolution. Am. Nat. 164:683–695.

Chatterton, B. D. E. 1980. Ontogenetic studies of Middle Ordovician trilobites from the Esbataottine Formation, Mackenzie Mountains, Canada. Palaeontographica, Abt. A 171:1–74.

Chatterton, B. D. E., D. J. Siveter, G. E. Edgecombe, and A. S. Hunt. 1990. Larvae and relationships of the Calymenina (Trilobita). J. Paleontol. 64:255–277.

Chatterton, B. D. E., and S. E. Speyer. 1997. Ontogeny. Pp. 173–247 *in* H. B. Whittington, ed. Treatise on Invertebrate paleontology, part O, Arthropoda 1. Trilobita, revised. Geological Society of America and Univ. of Kansas, Boulder and Lawrence.

Clarkson, E. N. K., J. Ahlgren, and C. M. Taylor. 2003. Structure, ontogeny, and moulting of the olenid trilobite *Ctenopyge (Eoctenopyge) angusta* Westergård, 1922 from the Upper Cambrian of Västergötland, Sweden. Palaeontology 46:1–27.

Cock, A. G. 1966. Genetical aspects of metrical growth and form in animals. Q. Rev. Biol. 41:131–190.

Cole, B. J. 1980. Growth ratios in holometabolous and hemimetabolous insects. Ann. Entomol. Soc. Am. 73:489–491.

Dyar, H. G. 1890. The number of molts in lepidopterous larvae. Psyche 5:420–422.

Ebach, M. C., and K. J. McNamara. 2002. A systematic revision of the family Harpetidae (Trilobita). Rec. Western Aust. Mus. 21:235–267.

Felsenstein, J. 1988. Phylogenies and quantitative characters. Annu. Rev. Ecol. Syst. 19:445–471.

———. 2008. Comparative methods with sampling error and within-species variation: contrasts revisited and revised. Am. Nat. 171:713–725.

Fortey, R. A. 1990. Ontogeny, hypostome attachment and trilobite classification. Palaeontology 33:529–576.

———. 1997. Classification. Pp. O289–302 *in* H. B. Whittington, ed. Treatise on invertebrate paleontology, part O, Arthropoda 1. Trilobita, revised. Geological Society of America and Univ. of Kansas, Boulder and Lawrence.

———. 2001. Trilobite systematics: the last 75 years. J. Paleontol. 75:1141–1151.

Fortey, R. A., and S. F. Morris. 1978. Discovery of nauplius-like trilobite larvae. Palaeontology 21:823–833.

Fusco, G. 2005. Trunk segment numbers and sequential segmentation in myriapods. Evol. Dev. 7:608–617.

Fusco, G., N. C. Hughes, M. Webster, and A. Minelli. 2004. Exploring developmental modes in a fossil arthropod: growth and trunk segmentation of the trilobite *Aulacopleura konincki*. Am. Nat. 163:167–183.

Garland, T., Jr., A. W. Dickerman, C. M. Janis, and J. A. Jones. 1993. Phylogenetic analysis of covariance by computer simulation. Syst. Biol. 42:265–292.

Gill, B. C., T. W. Lyons, S. A. Young, L. R. Kump, A. H. Knoll, and M. R. Saltzman. 2011. Geochemical evidence for widespread euxinia in the later Cambrian ocean. Nature 469:80–83.

Hansen, T. F. 1997. Stabilizing selection and the comparative analysis of adaptation. Evolution 51:1341–1351.

Harmon, L. J., J. Weir, C. Brock, R. Glor, W. Challenger, and G. Hunt. 2009. geiger: a package for macroevolutionary simulation and estimating parameters related to diversification from comparative phylogenetic data, Version 1.3-1. Avalable at http://cran.r-project.org/ (accessed April 13, 2011).

Harmon, L. J., J. B. Losos, T. J. Davies, R. G. Gillespie, J. L. Gittleman, W. B. Jennings, K. H. Kozak, M. A. McPeek, F. Moreno-Roark, T. J. Near, et al. 2010. Early bursts of body size and shape evolution are rare in comparative data. Evolution 64:2385–2396.

Hartnoll, R. G. 1982. Growth. Pp. 111–196 *in* L. G. Abele, ed. Embryology, morphology and genetics. Academic Press, New York.

Harvey, T. J. P., X. P. Dong, and P. C. J. Donoghue. 2010. Are palaeoscoleicids ancestral ecdysozoans? Evol. Dev. 12:177–200.

Hughes, N. C. 2007. The evolution of trilobite body patterning. Annu. Rev. Earth Planet. Sci. 35:401–434.

Hughes, N. C., A. Minelli, and G. Fusco. 2006. The ontogeny of trilobite segmentation: a comparative approach. Paleobiology 32: 602–627.

Hunt, G., and M. T. Carrano. 2010. Models and methods for analyzing phenotypic evolution in lineages and clades. Pp. 245–269 in J. Alroy and G. Hunt, eds. Quantitative methods in paleobiology. The Paleontological Society, New Haven.

Ives, A. R., P. E. Midford, and T. Garland, Jr. 2007. Within-species variation and measurement error in phylogenetic comparative methods. Syst. Biol. 56:252–270.

Klingenberg, C. P., and M. Zimmermann. 1992. Dyar's rule and multivariate allometric growth in nine species of waterstriders (Heteroptera: Gerridae). J. Zool. 227:453–464.

Lavin, S. R., W. H. Karasov, A. R. Ives, M. Middleton, and T. Garland, Jr. 2008. Morphometrics of the avian small intestine, compared with nonflying mammals: a phlyogenetic approach. Physiol. Biochem. Zool. 81: 526–550.

Lerosey-Aubril, R., and R. Feist. 2005. First Carboniferous protaspid larvae (Trilobita). J. Paleontology 79:702–718.

Lieberman, B. S., and T. S. Karim. 2010. Tracing the trilobite tree from the root to the tips: a model marriage of fossils and phylogeny. Arthropod Struct. Dev. 39:111–123.

Long, J. A., K. Trinajstic, and Z. Johanson. 2009. Devonian arthrodire embryos and the origin of internal fertilization in vertebrates. Nature 457:1124–1127.

Minelli, A., G. Fusco, and N. C. Hughes. 2003. Tagmata and segment specification in trilobites. Spec. Paper. Palaeontology 70:31–43.

Mosimann, J. E. 1970. Size allometry: size and shape variables with characterizations of the lognormal and generalized gamma distributions. J. Am. Stat. Assoc. 65:930–945.

Müller, G. B. 2007. Evo-devo: extending the evolutionary synthesis. Nat. Rev. Genet. 8:943–949.

Nijhout, H. F. 1994. Insect Hormones. Princeton Univ. Press, Princeton, NJ.

Pagel, M. 2002. Modelling the evolution of continuously varying characters on phylogenetic trees: the case of hominid cranial capacity. Pp. 269–286 in N. MacLeod and P. L. Forey, eds. Morphology, shape and phylogeny. Taylor & Francis, London.

Peters, S. E. 2007. The problem with the Paleozoic. Paleobiology 33:165–181.

Revell, L. J., L. J. Harmon, and D. C. Collar. 2008. Phylogenetic signal, evolutionary process, and rate. Syst. Biol. 57:591–601.

Rice, A. L. 1968. Growth rules and the larvae of decopod crustaceans. J. Nat. Hist. 2:525–530.

Salter, J. W. 1864. A monograph of British trilobites. Part 1. Palaeontographical Society, London, Monograph volume for 1862:1–80.

Smith, A. B. 2005. Growth and form in echinoids: the evolutionary interplay of plate accretion and plate addition. Pp. 181–195 in D. E. G. Briggs, ed. Evolving form and function: fossils and development. Peabody Museum of Natural History, Yale Univ., New Haven.

Speyer, S. E., and B. D. E. Chatterton. 1990. Trilobite larvae, larval ecology, and developmental paleobiology. Pp. 137–156 in D.G. Mikulic, ed.Short courses in paleontology Number 3. Paleontological Society, Knoxville, TN.

Stubblefield, C. J. 1926. Notes on the development of a trilobite, *Shumardia pusilla* (Sars). Zool. J. Linn. Soc. Lond. 35:345–372.

Waisfeld, B. G., N. E. Vaccari, G. D. Edgecombe, and B. D. E. Chatterton. 2001. Systematics of Shumardiidae (Trilobita), with new species from the Ordovician of Argentina. J. Paleontol. 75:827–859.

Waloszek, D., and A. Maas. 2005. The evolutionary history of crustacean segmentation: a fossil-based perspective. Evol. Dev. 7:515–527.

Webster, M., and M. L. Zelditch. 2011. Evolutionary lability of integration in Cambrian ptychoparioid trilobites. Evol. Biol. 38:144–162.

Associate Editor: C. Klingenberg

Supporting Information

The following supporting information is available for this article:

Table S1. Trilobite ontogeny dataset.

Table S2. Raw dataset with individual measurements for all species included and those excluded from analysis.

Figure S1. Developmental modes in trilobites.

Appendix S1. Estimation of *AGI* and *IDC* central value and dispersion statistics.

Appendix S2. Details on the construction of tree diagram.

Appendix S3. ASCII format data file used in phylogenetic signal and tree-based regression analyses.

Appendix S4. Possible taphonomic bias in the preservation of DM.

Supporting Information may be found in the online version of this article.

Please note: Wiley-Blackwell is not responsible for the content or functionality of any supporting information supplied by the authors. Any queries (other than missing material) should be directed to the corresponding author for the article.

Figure S1

Developmental modes in trilobites.
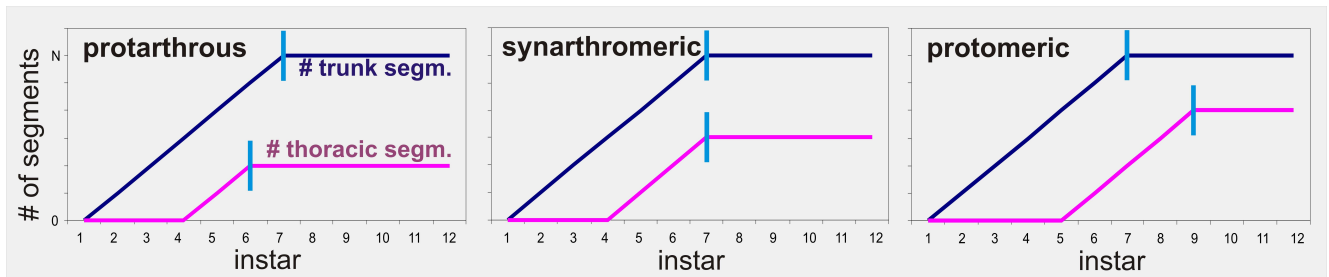
Developmental modes in trilobites. This classification combines aspects of ontogenetic change in trunk segment articulation (the traditional partition of trilobite ontogeny into the protaspid, meraspid, and holaspid phases) with the scheduling of trunk segment production (transition from the anamorphic phase, during which new trunk segments appeared at the rear of the trunk, to the epimorphic phase, during which the number of trunk segments remained constant). The three developmental modes are: *protarthrous*, in which the onset of the holaspid phase preceded onset of the epimorphic phase, *synarthromeric*, in case of synchronous onset of both phases, and *protomeric*, when onset of the epimorphic phase preceded the onset of the holaspid phase (details in Hughes N.C., Minelli A. & Fusco G. 2006. The ontogeny of trilobite segmentation: a comparative approach. *Paleobiology*, 32: 602-627).

Appendix S1

Estimation of *AGI* and *IDC* central value and dispersion statistics

1) *AGI* estimate

AGI is defined as

$$AGI = \frac{\overline{X}_N - \overline{X}_1}{N - 1}$$

where $\overline{X}_N$ and $\overline{X}_1$ are the mean logsize of the last (*N*th) and the first instars of the series, respectively, and *N* is the number of instars.

As *N* is a positive integer number, the problem of *AGI* estimation is that of the estimation of the difference between two independent random variables (the two sample means), both assumed with normal distribution. Thus, let define the variable Ψ as

$$\Psi = \overline{X}_N - \overline{X}_1$$

then, the central value of Ψ is estimated as the difference of the observed sample means values

$$\overline{\Psi} = \overline{X}_N - \overline{X}_1$$

and the standard deviation of Ψ is estimated as

$$s_\Psi = \sqrt{s_{\overline{X}_N}^2 + s_{\overline{X}_1}^2}$$

In the latter formula, $s_{\overline{X}}^2$ is the sample variance of the mean of the instar, estimated as

$$s_{\overline{X}}^2 = \left(\frac{s_X}{\sqrt{n}} C_n \right)^2$$

where s_X is the sample standard deviation, C_n is a correction factor (Gurland and Tripathi 1971) that accounts for the fact that *s* is a biased estimator of the parametric standard deviation (Sokal and Rohlf 1981), and *n* is the sample size of the instar.

2) *IDC* estimate

IDC is defined as

$$IDC = 1 - \frac{\left| \overline{X}_C - W_C \right|}{\rho(N-2)}$$

where $\overline{X}_C$ is the observed mean logsize of the instar (*C*th) that presents the maximum deviation from the corresponding expected mean logsize (W_C) under constant growth, ρ is the calculated average growth increment (*AGI*), and N is the number of instars. W_C is calculated as

$$W_C = \overline{X}_1 + (C-1)\frac{\overline{X}_N - \overline{X}_1}{N-1} = \overline{X}_1 + \left(\overline{X}_N - \overline{X}_1 \right)\frac{C-1}{N-1}$$

where $\overline{X}_1$ and $\overline{X}_N$ are the mean logsize of the first and the last (*N*th) instars of the series, respectively. We assume $\overline{X}_1 < \overline{X}_N$ and $\overline{X}_1 \leq \overline{X}_C \leq \overline{X}_N$

Expanding W_C and ρ in the first equation we have

$$IDC = 1 - \frac{\left| \overline{X}_C - \overline{X}_1 - \left(\overline{X}_N - \overline{X}_1 \right)\frac{C-1}{N-1} \right|}{\left(\overline{X}_N - \overline{X}_1 \right)\frac{N-2}{N-1}}$$

that simplifies to

$$IDC = 1 - \frac{N-1}{N-2}\left(\frac{\overline{X}_C - \overline{X}_1}{\overline{X}_N - \overline{X}_1} - \frac{C-1}{N-1} \right) \qquad \text{[for } \overline{X}_C > W_C\text{]}$$

or

$$IDC = 1 + \frac{N-1}{N-2}\left(\frac{\overline{X}_C - \overline{X}_1}{\overline{X}_N - \overline{X}_1} - \frac{C-1}{N-1} \right) \qquad \text{[for } \overline{X}_C < W_C\text{]}$$

Since C and N are both positive integer numbers, and not random variables, the problem of *IDC* estimation reduces to the estimation of the random variable θ, defined as

$$\theta = \frac{\overline{X}_C - \overline{X}_1}{\overline{X}_N - \overline{X}_1}$$

where X_1, X_C and X_N are assumed independent random variables with normal distribution and equal variance.

Let denoting with

$$t = t_{n_{X_1}+n_{X_C}+n_{X_N}-3,\alpha/2}$$

the proper percentile of Student distribution, and with

$$s_p^2 = \frac{\left(n_{X_1}-1\right)s_{X_1}^2 + \left(n_{X_C}-1\right)s_{X_C}^2 + \left(n_{X_N}-1\right)s_{X_N}^2}{n_{X_1}+n_{X_C}+n_{X_N}-3}$$

the pooled variance of the three variables X_1, X_C and X_N, where s_X^2 is the estimated variance of the variable and n is the size of the sample.

As $\dfrac{\overline{X}_C - \overline{X}_1 - \theta\left(\overline{X}_N - \overline{X}_1\right)}{s_p\sqrt{\dfrac{1}{n_{X_C}}+\dfrac{\theta^2}{n_{X_N}}+\dfrac{1-\theta^2}{n_{X_1}}}}$ has distribution $t_{n_{X_1}+n_{X_C}+n_{X_N}-3}$

for

$$\left(\overline{X}_N - \overline{X}_1\right)^2 > t\left(\frac{1}{n_{X_1}}+\frac{1}{n_{X_N}}\right)$$

the 1-α confidence interval of θ is given by

$$\hat{\theta} \pm e$$

where

$$\hat{\theta} = \frac{\left(\overline{X}_C - \overline{X}_1\right)\left(\overline{X}_N - \overline{X}_1\right) - \dfrac{t}{n_{X_1}} s_p^2}{\left(\overline{X}_N - \overline{X}_1\right)^2 - ts_p^2\left(\dfrac{1}{n_{X_1}} + \dfrac{1}{n_{X_N}}\right)}$$

and

$$e = \frac{\sqrt{\left[\left(\overline{X}_C - \overline{X}_1\right)\left(\overline{X}_N - \overline{X}_1\right) - \dfrac{t}{n_{X_1}} s_p^2\right]^2 - \left[\left(\overline{X}_C - \overline{X}_1\right)^2 - ts_p^2\left(\dfrac{1}{n_{X_1}} + \dfrac{1}{n_{X_C}}\right)\right]\left[\left(\overline{X}_N - \overline{X}_1\right)^2 - ts_p^2\left(\dfrac{1}{n_{X_1}} + \dfrac{1}{n_{X_N}}\right)\right]}}{\left(\overline{X}_N - \overline{X}_1\right)^2 - ts_p^2\left(\dfrac{1}{n_{X_1}} + \dfrac{1}{n_{X_N}}\right)}$$

References

Gurland, J. and R. C. Tripathi. 1971. A simple approximation for unbiased estimation of

the standard deviation. The American Statistician 25:30-32.

Sokal, R. R. and F. J. Rohlf. 1981. Biometry (II ed.). Freeman and Company, San

Francisco.

Appendix S2
Details on the construction of the tree diagram

We accept a monophyletic Trilobita (Edgecombe and Ramsköld 1999; Fortey and Whittington 1989) that roots near the base of the euarthropods (the group containing all living arthropods). For assessment of relationships between trilobites and other arthropods see: Budd (2002), Cotton and Braddy (2004), Edgecombe and Ramsköld (1999), Scholtz and Edgecombe (2005), and Walossek and Müller (1990). The trilobite body plan and developmental mode is likely to have been quite close to that of the euarthropod ancestor (Hughes 2005). Major trilobite clades that became dominant in the Ordovician and thereafter have long been recognised by systematists (e.g. Salter 1864). The principal challenge in trilobite phylogeny remains the identification of basal members of the major derived clades, (Eldredge 1977; Stubblefield 1959; Whittington 1981), and of the relationships among the stratigraphically earliest trilobites. The unresolved polytomies at the base of the tree, and among "libristomate" trilobites reflect this problem. However, provided that future work supports the monophyly of the major derived clades recognised herein, resolution of the basal polytomies would likely have limited influence of topology shown in Figure 3. This is because the majority of species included occupy relatively derived positions within their respective clades.

Olenelloidea, Agnostida, and "All other trilobites": Although the relationships among these clades are the subject of continuing debate (Lieberman and Karim 2010), the olenelloid species included in our analysis are all derived (Lieberman 1998) and are not considered part of a paraphyletic stem lineage of other trilobites. The same derived status applies to the agnostids included in our analysis: none considered are potential stem group members of other trilobite lineages. These facts, and the lack of the plesiomorphic non-olenelloid "redlichiid" trilobites in our sample, allows herein for a clear phylogenetic distinction between the olenelloids, agnostids, and all other trilobites.

Olenelloidea: Despite disagreement about the monophyly of olenelloid trilobites as a whole (e.g., Jell 2003), the species in our dataset belong to a monophyletic in-group of derived olenelloids (Lieberman 1998; Webster 2003). Relationships shown are based on Webster's (2003) phylogenetic analysis of olenelloid relationships. *Olenellus* species belong to the family Olenellidae, and *Nephrolenellus* to the Biceratopsidae, which are both derived families, as evinced by the markedly forward expanded glabella, that occur stratigraphically late within the range for the group. Olenelloids lack protaspid larvae, and thus did not contribute protaspid growth data to our analysis.

Agnostida: We accept Eodiscina and Agnostina as sister taxa, as supported by some authors (Cotton and Fortey 2005; Fortey and Whittington 1989), but rejected by others (Müller and Walossek 1987; Shergold 1991). Relationships within Eodiscina follow Jell (1997), who considered agnostinids to root among derived eodiscinids. We place *Neocobboldia chinlinica* as sister taxon to the agnostines on the basis of its wide axis, and also due to the marked similarity of other calodiscid cephala to those of agnostines. Agnostine protaspids are unknown and thus accepting eodiscine and agnostine monophyly has had no effect on our analysis of protaspid growth.

All other trilobites: The monophyly of "all other trilobites", though debated (Jell 2003), is accepted by most recent authors (e.g. Fortey 2001; Lieberman and Karim 2010). All non-agnostid and non-olenelloid trilobites are here treated as a clade, although relationships among these taxa are incompletely resolved. We follow Fortey (1990) in distinguishing Corynexochida and Lichida from other "libristomate" trilobites, and Chatterton and Speyer (1997) in considering these groups to be sister taxa (including odontopleurids as members of Lichida [Thomas and Holloway 1988]).

Corynexochida and Lichida: Similarities in the form of the protaspis may evince a relationship between derived corynexochide trilobites such as illaeninids and styginids, and lichids (see Fortey 2001, fig. 1). Basal corynexochides have a less distinctive protaspid morphology, but more derived forms bear other similarities to illaeninid and styginids (see Lee and Chatterton 2003; Zhu et al. 2010), and it is on this basis that we place the two scutelluid species as sister taxa to the Cambrian corynexochide *Bathyriscus fimbriatus*. Species of *Arthricocephalus* and *Duyunanaspis* form part of the distinctive oryctocephalid clade (Sundberg and McCollum 1997). Common ancestry between Lichoidea and Odontopleuroidea is suggested by the shared paired tubercle pattern in protaspid cephala and trunks, a marked anterior border, and marginal spines on the protaspid trunk (Thomas and Holloway 1988). We maintain this relationship because although more recent analysis questions this association (Campbell and Chatterton, 2009) it fails to provide a well-supported alternative hypothesis. Cambrian odontopleurids (e.g. Bruton 1983) differ markedly from corynexochide *Bathyriscus fimbriatus* and we root Lichida more basally, but with a long branch.

Libristomate trilobites: The grouping of "Ptychopariida", Asaphida, "Proetida" and Phacopida as a clade reflects Fortey's suggestion that the common ancestor of all these trilobites had a natant hypostome (Fortey 1990).

"Ptychopariida": Although Ptychopariida is evidently a paraphyletic group at best, a set of four ptychopariid trilobites (*G. parva, B. housensis, P. packi,* and *S. (C.) salopiensis*) included in our analysis have been treated as a clade, rather than placing them within the libristomate stem lineage. This association reflects the suggestion of F.A. Sundberg (pers. comm. 2007), but the their relationships to one another and to other trilobites are poorly resolved. Given the high variance in protaspid AGI seen within this "clade" (see Fig. 5) it seems unlikely that this grouping played a role in imparting the phylogenetic signal obtained. On the other hand, the Olenina do form a distinct "ptychopariid" clade that was specialized for life in dysaerobic environments (Fortey 1990; Lieberman and Karim 2010). Relationships among the families are poorly resolved, but the association of *Peltura* and *Ctenopyge* follows Henningsmoen (1957).

Asaphida: Synapomorphies for Asaphida include the median suture and asaphid protaspis (Fortey 1990; Fortey and Chatterton 1988). Although recent work has raised questions about asaphide monophyly (Adrain et al. 2009; Park and Choi 2010; Zhu et al. 2007; Zhu et al. 2010), these issues have little impact on the scheme in figure 3. This is because all the three asaphide taxa included in our dataset belong to the distinctive superfamily Trinucleoidea, whose relationships to other asaphides is unclear (Fortey 1990). Relationships among basal Trinucleoidea remain unresolved, but all members of the superfamily considered herein belong to genera that show a reduced number of thoracic segments and a triangular pygidium, putative trinucleoid synapomorphies (Vaccari et al. 2006). Here we consider the loss of the median glabellar spine and forward expanding glabella to unite the raphiophorid *Ampyxina bassleri* and the cryptolithid *Cryptolithus tesselatus,* which is a member of the derived family Trinucleidae.

Proetida: This order (Fortey and Owens 1975) comprises a large group of trilobite united by early protaspids with a developed frontal area and a fusiform glabella (Fortey 1990). Recent studies have revealed marked diversity among early ontogenetic stages of trilobites assigned to this group (Chatterton et al. 1999), although proetide monophyly has recently been supported (Lerosey-Aubril and Feist 2005), and we accept this herein. One proetide group, here represented by four members of the superfamily Proetoidea, has an initial inflated, "non adult-like" or "type A anaprotaspis" stage. Within this group *Osmolskabole prima* and *Drevermannia richteri* are united by thoracic segments that bear a preannulus, whilst the other Proetoidea lack this feature. Another major proetoid group has the "type B" protaspid, which is saucer shaped and bears a small hypostome. Proetide A may belong to this group, but is apparently plesiomorphic in other features, such as

lacking a frontal area (Lee and Chatterton 1997b), and is likely quite basal within the clade. Within the group with a "type B" protaspid there is a division into aulacopleuroid and bathyuroid trilobites, and among the aulacopleurids, which have the "B1" protaspid, the subtriangular glabella links *Lasarchopyge benedettoi* and *Scharyia micropyga*. *Hyperbolochilus* cf. *marginauctum* and "*Paraplethopeltis*" n. sp. are similar to aulacopleurids in having a type B protaspid, but differ in lacking later protaspids and early meraspids with paired tubercles. We place them in an unresolved position with regard to aulacopleuroids and bathyuroids. The form of the protaspid in the telephinid *T. problematica* suggests a link to the dimeropygids (R.M. Owens, pers, comm. 2007).

Phacopida: The division of Phacopida into calymenid, cheirurid, and phacopine trilobites is widely accepted (Fortey 1997), with the order united by an early protaspis with a distinctive pattern of marginal spines (Chatterton et al. 1990; Chatterton and Speyer 1997). Each clade is accepted to be monophyletic, with cheirurids and phacopines considered as sister taxa (Fortey 1990) on the basis of sharing proparian sutures and forward expanding glabella. Cheirurine monophyly is supported by marginal pygidial spines and a specific type of thoracic articulation (Fortey 1990), but others have considered Cheirurina as a paraphyletic group (Edgecombe 1992). Among the calymenids in our sample the homalonotid *Brongniartella* sp. is placed as a sister taxon to the calymenids *Flexicalymene senaria* and *Diacalymene gabrielsi* according to Chatterton et al. (1990). Relationships within the cheirurids are presently less well resolved (see Lieberman and Karim 2010). The monophyly of the encrinurids *(Avalanchurus lennoni* and *Physemataspis insularis)* is well established (Edgecombe et al. 1988), as is their relationship between cybelines *Lyrapyge ebriosus* and *Cybelurus halo* (Lee and Chatterton 1997a). Placement of *Rossaspis pliomeris* as basal to that clade is based on its sharing the pitted protaspid fixigenal field. *Tesselacauda depressa* and *Ceraurinella chandra* share holaspid pygidial pleural furrows, and all these trilobites are distinguished from other cheirurids by the series of characters outlined by Lee and Chatterton (1997a), who distinguished a grade among pliomerid trilobites the sequence of which formed the basis of the relationships shown herein. The phacopine trilobites included in this analysis are all derived and stratigraphically late members of the family Phacopidae, characterized by wide glabellae (Ramsköld and Werdelin 1991). *Weyerites ensea* is considered the sister taxon to the two *Trimerocephalus* species based on the shared reduction of the eye size (Crônier et al. 1998; Osmólska 1963), and these taxa share with *Eldredgeops milleri* ankylosis of the dorsal sutures in the holaspid phase (Crônier et al. 1999). *Nephranops incisus incisus* lacks this character and is thus placed as basal within this clade, although glabellar structure and eye reduction may imply a closer relationship to *Weyerites ensea* and the *Trimerocephalus* species.

Stratigraphic Age and Branch Length Estimation: Age estimates for species in the dataset were based on the correlation of biostratigraphically determined stratigraphic age estimates with the recent *Concise Geological Timescale* (Ogg et al. 2008). Trilobita had a history that extended prior to the earliest known of their fossils, and it is possible that the lineages bearing olenelloids and agnostids diverged significantly earlier than shown in Fig 3. Divergences among "all other trilobites" in our sample likely took place within the Cambrian and thereafter (Hughes 2007). Branch length estimates were determined in various ways. Stratigraphic information about sister taxon ages determined branching age, and single long branches where preferred in cases where "ghost lineages" are inferred (see Edgecombe 1994). Notable examples of ghost lineages in our sample include styginid, drevomanid, and phacopinid clades, but in some cases long branches were complemented by the stratigraphic occurrence of basal representatives of these clades coincident with the inferred branching age (examples including putative Cambrian cheirurines [Rozova 1960] and odontopleurids [Bruton 1983]). Node dates were calculated either from cases in which phylogenies have been mapped onto stratigraphic occurrence (e.g., Lee and Chatterton 1997), or from data on the first appearance of basal members of the clade.

Adrain, J. M., S. E. Peters, and S. R. Westrop. 2009. The Marjuman trilobite Cedarina Lochman: thoracic morphology, systematics, and new species from western Utah and eastern Nevada, USA. Zootaxa 2218: 38-58.

Bruton, D. 1983. Cambrian origins of the odontopleurid trilobites. Palaeontology 26:875-885.

Budd, G. E. 2002. A palaeontological solution to the arthropod head problem. Nature 417:271-275.

Campbell, M. J., and B. D. E. Chatterton. 2009. Silurian lichid trilobites from Northwestern Canada: Ontogeny and Phylogeny of Lichids. Journal of Paleontology 83:263-279.

Chatterton, B. D. E., G. D. Edgecombe, N. E. Vaccari, and B. G. Waisfeld. 1999. Ontogenies of some Ordovician Telephinidae from Argentina and larval patterns in the Proetida (Trilobita). Journal of Paleontology 73:219-239.

Chatterton, B. D. E., D. J. Siveter, G. E. Edgecombe, and A. S. Hunt. 1990. Larvae and relationships of the Calymenina (Trilobita). Journal of Paleontology 64:255-277.

Chatterton, B. D. E., and S. E. Speyer. 1997. Ontogeny. Pp. 173-247 in H. B. Whittington, ed. Treatise on Invertebrate Paleontology, part O, Arthropoda 1. Trilobita, revised. Geological Society of America and University of Kansas, Boulder and Lawrence.

Cotton, T. J., and S. J. Braddy. 2004. The phylogeny of arachnomorph arthropods and the origin of the Chelicerata. Transactions of the Royal Society of Edinburgh, Earth Sciences 94 (for 2003):169-193.

Cotton, T. J., and R. A. Fortey. 2005. Comparative morphology and relationships of the Agnostida. Pp. 95-136 in S. Koenemann and R. A. Jenner, eds. Crustacean Issues 16. Crustacea and arthropod phylogeny. CRC Press, Boca Raton, Florida.

Crônier, C., K. Bartzsch, D. Weyer, and R. Feist. 1999. Larval morphology and ontogeny of a late Devonian phacopid with reduced sight from Thuringia, Germany. Journal of Paleontology 73:240-255.

Crônier, C., S. Renaud, R. Feist, and J.-C. Auffray. 1998. Ontogeny of *Trimerocephalus levievrei* (Trilobita, Phacopida), a representative of the Late Devonian phacopine paedomorphocline: a morphometric approach. Paleobiology 24:359-370.

Edgecombe, G. D. 1992. Trilobite phylogeny and the Cambrian-Ordovician "Event": Cladistic reappraisal. Pp. 144-177 in M. J. Novacek and Q. D. Wheeler, eds. Extinction and Phylogeny. Columbia University Press, New York.

Edgecombe, G. D. 1994. New Lower Silurian (Llandovery) encrinurine trilobites from the Mackenzie Mountains, Canada. Journal of Paleontology 68:824-837.

Edgecombe, G. D., and L. Ramsköld. 1999. Relationships of Cambrian Arachnata and the systematic position of Trilobita. Journal of Paleontology 73:263-287.

Edgecombe, G. D., S. E. Speyer, and B. D. E. Chatterton. 1988. Protaspid larvae and phylogenetics of encrinurid trilobites. Journal of Paleontology 62:779-799.

Eldredge, N. 1977. Trilobites and evolutionary patterns. Pp. 305-332 in A. Hallam, ed. Patterns of evolution. Elsevier, Amsterdam.

Fortey, R. A. 1990. Ontogeny, hypostome attachment and trilobite classification. Palaeontology 33:529-576.

Fortey, R. A. 1997. Classification. Pp. O289-302 in H. B. Whittington, ed. Treatise on Invertebrate Paleontology, part O, Arthropoda 1. Trilobita, revised. Geological Society of America and University of Kansas, Boulder and Lawrence.

Fortey, R. A. 2001. Trilobite systematics: the last 75 years. Journal of Paleontology 75:1141-1151.

Fortey, R. A., and B. D. E. Chatterton. 1988. Classification of the trilobite suborder Asaphina. Palaeontology 31:165-222.

Fortey, R. A., and R. M. Owens. 1975. Proetida - a new order of trilobites. Fossils and Strata 4:227-239.

Fortey, R. A., and H. B. Whittington. 1989. The Trilobita as a natural group. Historical Biology 2:125-138.

Henningsmoen, G. 1957. The Trilobite family Olenidae. Skrifter Utgitt av Det Norske Videnskaps-Akademi i Oslo 1. Matematisk - Naturvidenskabelig Klasse 1:1-303.

Hughes, N. C. 2005. Trilobite construction: building a bridge across the micro and macroevolutionary divide. Pp. 138-158 in D. E. G. Briggs, ed. Evolving Form and Function: Fossils and Development. Peabody Museum of Natural History, Yale University, New Haven.

Hughes, N. C. 2007. The evolution of trilobite body patterning. Annual Reviews of Earth and Planetary Sciences 35:401-434.

Jell, P. A. 1997. Introduction to the suborder Eodiscina. Pp. O384-O404 in H. B. Whittington, ed. Treatise on Invertebrate Paleontology, part O, Arthropoda 1. Trilobita, revised. Geological Society of America and University of Kansas, Boulder and Lawrence.

Jell, P. A. 2003. Phylogeny of early Cambrian trilobites. Special Papers in Palaeontology 70:45-57.

Lee, D.-C., and B. D. E. Chatterton. 1997a. Ontogenies of trilobites from the lower Ordovician Garden City Formation of Idaho and their implications for the phylogeny of the Cheirurina. Journal of Paleontology 71:683-702.

Lee, D.-C., and B. D. E. Chatterton. 1997b. Three new proetide trilobite larvae from the Lower Ordovician Garden City Formation in southern Idaho. Journal of Paleontology 71:434-441.

Lee, D.-C., and B. D. E. Chatterton. 2003. Protaspides of Leiostegium and their implications for membership of the order Corynexochida. Palaeontology 46:431-445.

Lerosey-Aubril, R., and R. Feist. 2005. First Carboniferous protaspid larvae (Trilobita). Journal of Paleontology 79:702-718.

Lieberman, B. S. 1998. Cladistic analysis of the early Cambrian olenelloid trilobites. Journal of Paleontology 72:59-78.

Lieberman, B. S., and T. S. Karim. 2010. Tracing the trilobite tree from the root to the tips: a model marriage of fossils and phylogeny. Arthropod Structure and Development 39:111-123.

Müller, K. J., and D. Walossek. 1987. Morphology, ontogeny, and life habit of Agnostus pisiformis from the Upper Cambrian of Sweden. Fossils and Strata 19:1-124.

Ogg, J. G., G. Ogg, and F. M. Gradstein. 2008. The Concise Geological Timescale. Cambridge University Press, Cambridge.

Osmólska, H. 1963. On some Famennian Phacopinae (Trilobita) from the Holy Cross Mountains (Poland). Acta Palaeontologica Polonica 8:495-523.

Park, T.-Y., and D. K. Choi. 2010. Ontogeny of the Furongian (late Cambrian) remopleuridioid trilobite Haniwa quadrata Kobayashi, 1933 from Korea: implications for trilobite taxonomy. Geological Magazine

Ramsköld, L., and L. Werdelin. 1991. The phylogeny and evolution of some phacopid trilobites. Cladistics 7:29-74.

Rozova, A. V. 1960. The Upper Cambrian Trilobita of Salair (Verkhnekembriiskia trilobity Salaira). Trudy Institut geologii i geofiziki, Sibirskoe otdeleniye, Akademiya nauk SSSR. 116:1-116.

Salter, J. W. 1864. A monograph of British trilobites. Part 1. Palaeontographical Society, London, Monograph volume for 1862:1-80.

Scholtz, G., and G. D. Edgecombe. 2005. Heads, Hox, and the phylogenetic position of trilobites. Pp. 139-165 in S. Koenemann and R. A. Jenner, eds. Crustacean Issues 16. Crustacea and Arthropod Phylogeny. CRC Press, Boca Raton, Florida.

Shergold, J. H. 1991. Protaspid and early meraspid growth stages of the eodiscoid trilobite Pagetia ocellata Jell, and their implications for classification. Alcheringa 15:65-86.

Stubblefield, C. J. 1959. Evolution in trilobites. Journal of the Geological Society of London 115:145-162.

Sundberg, F. J., and L. B. McCollum. 1997. Oryctocephalids (Corynexochida: Trilobita) of the Lower-Middle Cambrian boundary interval from California and Nevada. Journal of Paleontology 71:1065-1090.

Thomas, A. T., and D. J. Holloway. 1988. Classification and phylogeny of the trilobite order Lichida. Philosophical Transactions of the Royal Society of London. B. Biological Sciences 321:179-262.

Vaccari, N. E., B. G. Waisfeld, B. D. E. Chatterton, and G. E. Edgecombe. 2006. New raphiophorid trilobites from the Ordovician of Argentina and their biogeographic implications. Memoirs of the Association of Australasian Palaeontologists 32:353-374.

Walossek, D., and K. J. Müller. 1990. Upper Cambrian stem-lineage crustaceans and their bearing on the monophyletic origin of Crustacea and the position of *Agnostus*. Lethaia 23:409-427.

Webster, M. 2003. Ontogeny and Phylogeny of Early Cambrian Olenelloid Trilobites, with Emphsis on the late Dyeran Biceratopsidae. Pp. 538. Earth Sciences. University of California, Riverside.

Whittington, H. B. 1981. Paedomorphosis and cryptogenesis in trilobites. Geological Magazine 18:591-602.

Zhu, X., N. C. Hughes, and S. Peng. 2007. On a new species of *Shergoldia* Zhang and Jell, 1987 (Trilobita), the family Tsinaniidae and the order Asaphida. Memoirs of the Association of Australasian Palaeontologists 34:243-253.

Zhu, X., N. C. Hughes, and S. Peng. 2010. Ventral structure and ontogeny of the late Furongian (Cambrian) trilobite *Guangxiaspis guangxiensis* Zhou 1977 and the diphyletic origin of the median suture. Journal of Paleontology 84:492-503.

Appendix S4. Possible taphonomic bias in the preservation of DM.

In our sample all three developmental modes are equally represented in deeper water environments, but protomeric development overwhelmingly dominated in shallow water environments. In lower energy, deeper water settings, complete exoskeletons are preserved more commonly, permitting the recognition of all three modes of development with comparable probability. Exoskeletal disarticulation is common in materials from shallow water because of greater wave and current agitation in the shallow seafloor. In case of disarticulated material, protomeric development can be recognized with more confidence from pygidia alone than the other two developmental modes. This is because in protomeric development late stage meraspid pygidia were characterized by a progressive reduction in segment number, with the mature pygidium always having the smallest number of segments, whereas in synarthromeric growth late stage meraspids and holaspids had the same number of segments, and are thus indistinguishable in disarticulated material. In protarthrous development pygidial segment number increased from late stage meraspids to early holaspids, but as the pattern of segment accretion was commonly inconstant during this interval (see Hughes et al. 2006, figs. 4B,C), detecting protarthrous development in disarticulated material presents a greater challenge. For these reasons it is practically easier to recognize protomeric development in disarticulated materials in which multiple late meraspid instars are present. Disarticulated material is more common in shallower settings. Accordingly, the preponderance of this condition in this setting could be taphonomic, as opposed to biological, in origin.